THE ASTROPHYSICAL JOURNAL, 241:736–758, 1980 October 15

THE CHEMICAL COMPOSITION, GRAVITY, AND TEMPERATURE OF VEGA[1]

L. A. DREILING
Lawrence Livermore Laboratory, University of California

AND

R. A. BELL[2]
Laboratory for Astronomy and Solar Physics, NASA Goddard Space Flight Center
Received 1979 February 12; accepted 1980 April 18

ABSTRACT

Several flux-constant, line-blanketed model stellar atmospheres have been computed for the bright star Vega. The stellar effective temperature has been found to be 9650 K by comparisons of observed and computed absolute fluxes at 5556 Å and of relative absolute fluxes between 3300 and 10800 Å. The Balmer line profiles give log $g=3.9\pm0.2$, consistent with the result from the Balmer jump and with that found from the radius and (estimated) mass. The Ti II and Fe II curves of growth give abundances of log $N(\mathrm{Ti})=4.7\pm0.3$ and log $N(\mathrm{Fe})=7.1\pm0.3$ on the scale log $N(\mathrm{H})=12.0$. These abundances are slightly less than normalized meteoritic values and solar values deduced from ionized lines. The local thermodynamic equilibrium (LTE) Fe I curve of growth gives log $N(\mathrm{Fe})=6.9\pm0.3$, whereas correction for non-LTE effects suggests log $N(\mathrm{Fe})=7.5\pm0.3$.

The model fluxes between 1200 and 3300 Å generally agree with observations of Vega from satellites and can be regarded as giving an independent calibration of the satellite fluxes. Infrared model fluxes have been computed between 1 and 30 μm and these provide a calibration of airborne and ground-based photometry.

Subject headings: stars: abundances — stars: atmospheres — stars: early-type — stars: individual

I. INTRODUCTION

The bright star Vega (αLyr, HR 7001, HD 172167) has been studied extensively in recent years because it serves as the primary standard star for photoelectric spectrophotometry. Measurements of the absolute energy distribution in the visible and near-infrared regions of the spectrum have been carried out by Hayes (1970), Oke and Schild (1970), Hayes and Latham (1975), Hayes, Latham, and Hayes (1975), and Tüg, White, and Lockwood (1977). The ultraviolet flux has been studied using the *OAO* 2 satellite (Code and Meade 1976) and the S2/68 experiment on the *TD* 1 satellite (Malaise, Gros, and Macau 1974). The infrared flux between 1.2 and 5.5 μm has been studied by the NASA Ames group (Augason *et al.* 1977). Hunger (1955) has measured equivalent widths of lines in the visible spectrum. Faraggiana, Hack, and Leckrone (1976) have used the *Copernicus* satellite to observe the line spectrum between 1100 and 1740 Å and 2000 and 3000 Å, at resolutions of 0.2 and 0.4 Å, respectively. These authors identified spectral lines and gave line depths and blocking coefficients. Hydrogen Balmer-line profiles have been published by Peterson (1969), Gray and Evans (1973), and others. Hydrogen Paschen α and β and Brackett lines have been seen in infrared data (McCammon, Münch, and Neugebauer 1966; Johnson and Méndez 1970; Augason *et al.* 1977; Strecker, Erickson, and Witteborn 1979, Ridgway 1978).

Analyses of the information available have been carried out by Hunger (1955), Strom, Gingerich, and Strom (1966), and Gehlich (1969), all of whom used equivalent widths to derive chemical abundances. The ground-based spectrophotometry of Vega has been studied to determine the effective temperature, e.g., by Schild, Peterson, and Oke (1971), Kurucz (1975), and Panek (1977), who also used the *OAO* 2 data. Kurucz (1979) has also made detailed comparisons of his models with ground based observations of Vega.

For the following reasons, we felt it desirable to further analyze Vega. First, the information now available on the ultraviolet spectrum is extensive and ripe for comparison with model predictions. Second, recent measurements of accurate oscillator strengths and equivalent widths should make it possible to determine abundances more reliably. Third, it is currently possible to study non-LTE effects both in the calculations of stellar model atmospheres and in line formation calculations, and we wish to determine if the predictions are

[1] This work was performed under the auspices of the U.S. Department of Energy by Lawrence Livermore Laboratory under contract W-7405-Eng-48.

[2] On sabbatical from the University of Maryland, Astronomy Program.

confirmed observationally. Fourth, in analyzing the colors of model atmospheres for cool stars (Gustafsson and Bell 1979), the observed and calculated colors for Vega have been very valuable; therefore, it is important to have the best possible Vega model for calculated colors. Fifth, infrared observers are using Vega as a calibration object for photometry of cool stars (Nordh, Olofsson, and Augason 1978), and theoretical fluxes are needed to interpret this photometry.

II. OBSERVATIONS

Hayes and Latham (1975) have used the infrared flux measurements of Hayes, Latham and Hayes (1975), made at Mount Hopkins, and the earlier absolute calibrations of Hayes (1970) and of Oke and Schild (1970, made at Mount Palomar) to obtain an absolute-flux calibration. The main improvement by Hayes and Latham lies in their treatment of the effects of atmospheric extinction. They quote an absolute flux at 5556 Å of $F_{5556}=3.39\times10^{-9}$ ergs cm^{-2} s^{-1} Å^{-1} as the average of the two sets of data. The Mount Hopkins value is the larger of the two, being 3.45×10^{-9} ergs cm^{-2} s^{-2} Å^{-1}. The Hayes, Latham, and Hayes flux at 10,400 Å is 5.70×10^{-10} ergs cm^{-2} s^{-1} Å^{-1} with an estimated error of 2% and the color $m_\lambda(8090)-m_\lambda(10400)=-0.703$, with an error of ±0.01 mag.

The most recent absolute calibration of the visual flux from Vega is that of Tüg, White, and Lockwood (1977). These authors measured fluxes every 50 Å, with band passes of 10Å between 3295 and 5695 Å and 20 Å between 4990 and 9040 Å. For calibration purposes, they used portable blackbodies operating at the melting points of copper and platinum. They stated that the use of these devices avoids the problems associated with the standard lamps used in some earlier calibration work. The fluxes measured are thought to be accurate within ±0.02 mag between 3300 and 4000 Å and within ±0.01 mag between 4000 and 9000 Å. The absolute visible flux at 5556 Å is quoted as $F_{5556}=3.47\times10^{-9}$ ergs cm^{-2} s^{-1} Å^{-1}, about 2% greater than the adopted value of Hayes and Latham and less than 1% greater than the Mount Hopkins value. If the Tüg *et al.* fluxes are interpolated to the individual wavelengths of the Hayes and Latham calibration, the average difference is quoted by Tüg *et al.* as 0.006 mag (the Tüg values being brighter) with an RMS value of 0.014 mag.

Code and Meade (1976) obtained data on Vega using the two spectrum scanners of the Wisconsin Experiment package on the *OAO* 2 satellite. The spectral resolution of the tabulated fluxes is approximately 12 Å between 1160 and 1850 Å and 22 Å between 1850 and 3600 Å. The mean error reported for the ultraviolet flux calibrations is $\pm21\%$ for $\lambda<1850$ Å and $\pm8.5\%$ for $1850<\lambda<3300$ Å although Bohlin *et al.* (1980) have argued that the Code and Meade fluxes are generally too great in the wavelength region 1200–1900 Å by up to a factor of 1.25.

These absolute fluxes were converted to emergent fluxes at the surface of Vega by multiplying by the geometrical dilution $(d/R)^2$, given by

$$\frac{d}{R}=\frac{2.06265\times10^5}{\theta_{\rm LD}/2},$$

TABLE 1

OBSERVED EQUIVALENT WIDTHS

λ	log W/λ	log $gf\lambda$	χ
Fe I Lines			
4005.25....	−5.04	3.23	1.56
4045.82....	−4.74	4.04	1.49
4063.60....	−4.83	3.88	1.56
4071.74....	−4.92	3.78	1.61
4187.80....	−5.38	3.13	2.43
4202.83....	−5.13	3.07	1.49
4250.13....	−5.37	3.43	2.45
4250.79....	−5.23	3.09	1.55
4260.48....	−5.05	3.96	2.38
4271.76....	−4.91	3.65	1.47
4282.41....	−5.34	3.06	2.16
4299.24....	−5.35	3.50	2.43
4383.55[a]...	−4.75	3.96	1.47
4404.75....	−4.91	3.64	1.55
Fe II Lines			
4489.19....	−5.18	0.64	2.81
4491.40....	−5.08	0.93	2.83
4508.28....	−4.83	1.08	2.83
4515.34....	−4.87	1.12	2.82
4520.23....	−4.97	0.93	2.78
4522.63....	−4.88	1.19	2.82
4541.52....	−5.26	0.58	2.83
4555.89....	−4.85	1.01	2.81
4576.33....	−5.17	0.49	2.82
4582.84....	−5.36	0.27	2.82
4583.83....	−4.72	1.58	2.78
4629.34....	−4.92	1.11	2.78
4666.75....	−5.39	0.10	2.81
Ti II Lines			
4028.33....	−5.17	2.49	1.88
4163.64....	−5.02	3.22	2.57
4171.90....	−5.04	3.06	2.58
4290.22....	−4.90	2.47	1.15
4395.03....	−4.78	2.99	1.07
4399.77....	−5.14	2.13	1.23
4417.72....	−5.09	2.28	1.15
4443.80....	−4.82	2.84	1.07
4450.49....	−5.28	2.06	1.07
4468.49....	−4.83	2.88	1.12
4501.27....	−4.87	2.79	1.11
4533.97....	−4.76	2.95	1.23
4563.76....	−4.90	2.76	1.21
4571.97....	−4.79	3.01	1.56

[a] The sign of the reported value (log gf = −0.32) appears to be a typographical error.

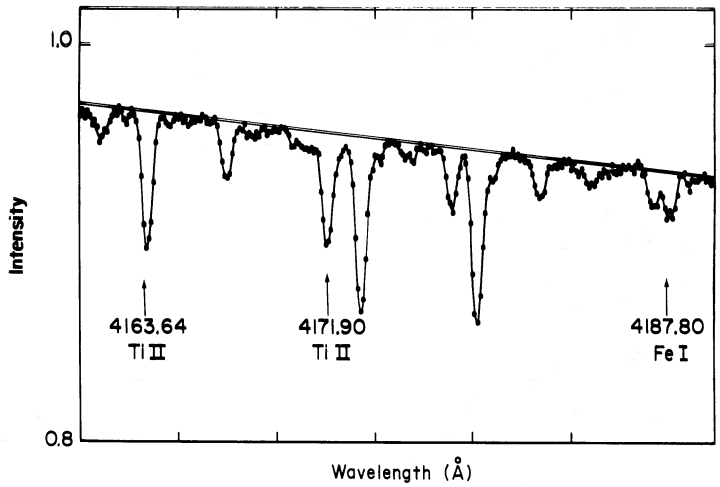

FIG. 1.—A region of the observed Vega spectrum obtained with a signal-to-noise ratio of better than 900 and a resolution of 0.2–0.3 Å. Lines measured are identified.

where d is the distance to Vega, R the radius of Vega, and θ_{LD} the stellar angular diameter in seconds of arc corrected for limb darkening. Hanbury Brown, Davis, and Allen (1974) gave $\theta_{LD}=(3''24\pm0.07)\times10^{-3}$, yielding $(d/R)^2=(1.62\pm0.03)\times10^{16}$. The data of Tüg, White, and Lockwood (1977) then yielded an absolute flux of $(5.625\pm0.243)\times10^7$ ergs cm^{-2} s^{-1} Å^{-1} at 5556 Å. The estimated error comes from the errors of 2% in both the flux and the angular diameter.

Another parameter needed to calculate a model atmosphere is the surface gravity, which can be estimated only approximately for Vega. The parallax of Vega is $0''123\pm0''005$ (Jenkins 1963), and combining this with θ_{LD} we find a stellar radius of 1.97×10^{11} cm. Since Vega and Sirius A have spectral types of A0 V and A1 V, respectively, we feel their masses should be very similar and assume the mass of Vega is 2.0 $M_\odot$ (the mass of Sirius A is 2.1 $M_\odot$) and then find log $g=3.83$, with g in cgs units. Uncertainties in θ_{LD}, π, and the mass probably cause a total uncertainty of $\pm40\%$ in g or 0.15 in log g.

Through the kindness of D. L. Lambert, we were able to observe Vega with the McDonald Observatory's 2.7 m reflector and the Tull coudé spectrograph equipped with a 1024 element Reticon array (Vogt, Tull, and Kelton 1978). The observations, covering the wavelength interval 4000–5000 Å, were obtained with a grating providing 100 Å of spectrum at a resolution of 0.2 to 0.3 Å, and a signal-to-noise ratio of 900 or better. A further series of six spectra, each covering 50 Å in the range 4100–4600 Å with a resolution of 0.1–0.15 Å, and a signal-to-noise ratio of 600 or better was ob-

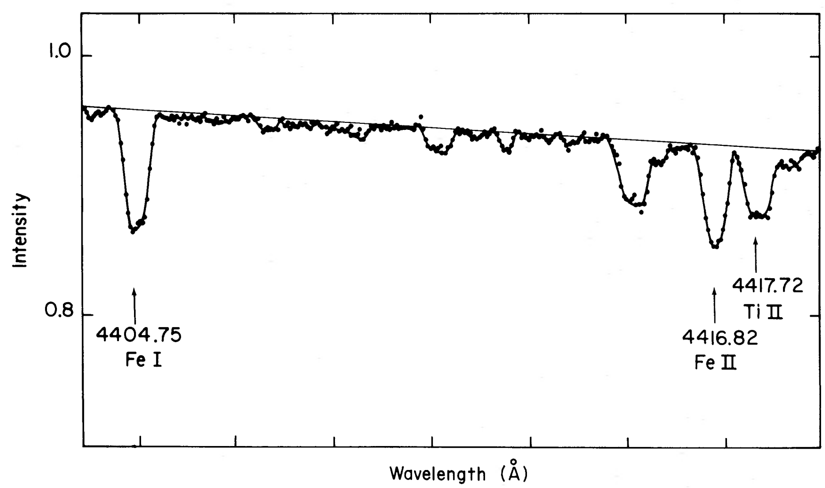

FIG. 2.—As Fig. 1, the signal to noise being better than 600 and the resolution being 0.1–0.15 Å

tained with the same equipment by R. E. S. Clegg. Equivalent widths of Fe I, Fe II, and Ti II lines measured from these spectra are given in Table 1. Examples of the spectra are given in Figures 1 and 2. The equivalent widths should be much more accurate than those of Hunger (1955), which were obtained from several spectra, some of relatively low dispersion. Our values are, on average, about 75% of Hunger's. An analysis of these data is presented in § IV*d*. The results found from Hunger's data are also given.

III. CALCULATIONS OF MODEL ATMOSPHERES

We used the computer program MARCS to calculate model stellar atmospheres for Vega. This program was used earlier to compute a grid of flux-constant, line-blanketed models for cool stars. The techniques used by the program and the sources of data were discussed by Gustafsson *et al.* (1975). Because the Vega models are much hotter than the models computed in that work, it was necessary to make some minor modifications to the program. The only additional continuous-opacity source added was He I, the data being taken from Peach (1970).

The effects of bound-bound opacity are included in MARCS through the use of opacity distribution functions (ODFs). Gustafsson *et al.* (1975) used 368 points to describe the radiation field in their models: eight points in the ODF regions ≤ 2076 Å, 176 points in the ODF regions between 2076 and 7200 Å, and 184 points in the ODF regions between 7200 and 130000 Å. They constructed more accurate ODFs for $\lambda > 3000$ Å than for $\lambda < 3000$ Å. For example, they assumed the line absorption in the interval 2076–2515 Å was that of the interval 3000–3100 Å. Such approximations, which seem quite adequate for cool stars, could not be made in the present work because a far greater fraction of the stellar flux is in the ultraviolet.

Therefore, we searched the literature for further sources of laboratory data on spectral lines in the ultraviolet. We initially used the measurements of Banfield and Huber (1973) for 104 lines of Fe I between 2084 and 3194 Å. These lines were used to find intensity-dependent and wavelength-dependent corrections (Bell and Upson 1971; Dreiling 1976), which then were applied to the Fe I line data of Corliss and Tech (1968). This gave data for an additional 450 Fe I lines between 2080 and 3000 Å. We used the laboratory Fe II *gf* values of Corliss and Bozman (1962), Warner (1967), and Huber (1974) and similarly corrected the older values to the scale of the most recent. The ultraviolet line data on other elements were taken from Corliss and Bozman (1962), Warner (1967), Wiese, Smith, and Glennon (1966), Wiese, Smith, and Miles (1969), Roberts, Anderson, and Sørensen (1973*a*, *b*), Garz (1973), Roberts, Voigt, and Czernichowski (1975), and Goly, Moity, and Weniger (1975).

Comparing a synthetic spectrum for Sirius with observational data obtained using the *Copernicus* satellite (Dreiling 1976), we found it necessary to add still further atomic lines to our data base. For this purpose we used only the very comprehensive set of atomic line data published by Kurucz and Peytremann (1975) for wavelengths below 2695 Å and, for simplicity, rejected the laboratory data at shorter wavelengths.

Edmonds, Schlüter, and Wells (1967) have published Stark broadening functions for hydrogen lines of the Lyman, Balmer, and Paschen series. These functions were convolved with Voigt functions that took into account Doppler, natural, and resonance broadening (Dreiling 1976). The resultant absorption coefficients were included in the ODF calculations. In our work on Brackett lines, we have considered only the Stark broadening, using the Edmonds, Schlüter, and Wells results. Although the Brackett lines were not included in ODF calculations, they were used in synthetic spectrum work. The Vidal, Cooper, and Smith (1973) Stark broadening calculations are discussed subsequently.

The synthetic spectrum program SSG (Bell and Gustafsson 1978) was used to compute the ODFs from the atomic and hydrogen line data. We computed the line absorption as a function of temperature and electron pressure every 0.05 Å from 1200 to 7200 Å. We computed 60 ODFs (each 100 Å wide) from the line absorption coefficients, using four wavelength points per ODF. The line absorption is small at wavelengths greater than 7200 Å, except for the Paschen lines. However, to avoid programming changes to MARCS, we computed an additional 184 ODFs for the wavelength range 7200–130000 Å, following Gustafsson *et al.* (1975). Thus, a total of 424 wavelength points was used in the calculation of the Vega models.

We calculated two complete sets of ODFs. In the first set we used solar abundances, and in the second set we enhanced these abundances for all metals by a factor of 3 relative to H and He. The metal-rich ODFs were intended primarily for use in analyses of Sirius, but we used them in our studies of Vega. The Doppler-broadening velocity was taken to be 3 km s^{-1}, based on the Fe I curve of growth for Sirius (Dreiling 1976). The main contributor to line broadening in these calculations is natural broadening, for which we used $\Gamma_{\rm nat} = 1.13 \times 10^8$ for all lines. This corresponds to a value of the damping constant $a = 0.0017$ at 5000 Å. A more detailed discussion of the damping treatment and a table of abundances we used are given by Bell and Gustafsson (1978). The only difference between the version of the SSG program used here and that used by Bell and Gustafsson is that we took the values of the continuous absorption coefficients for C I, Mg I, Al I, and Si I from Peach (1970). Bell and Gustafsson, neglecting C I, used the Travis and Matsushima (1968) data for Mg I, Fe I, and Si I.

TABLE 2

CHARACTERISTICS OF ADOPTED VEGA MODEL (9650/3.9/0.0)

τ(Ross)	T	log P	log P_e	μ	κ(Ross)
0.0000E−00 ...	6877.2	1.1301	0.0773	1.179	0.1106
1.0000E−04 ...	6984.9	1.1128	0.1430	1.155	0.1169
1.4678E−04 ...	7030.1	1.2037	0.2248	1.158	0.1266
2.1544E−04 ...	7078.0	1.3044	0.3134	1.162	0.1383
3.1623E−04 ...	7130.6	1.4090	0.4071	1.165	0.1535
4.6416E−04 ...	7195.6	1.5158	0.5094	1.166	0.1756
6.8129E−04 ...	7254.8	1.6234	0.6077	1.169	0.1995
1.0000E−03 ...	7316.8	1.7301	0.7067	1.171	0.2289
1.4678E−03 ...	7378.2	1.8369	0.8047	1.174	0.2634
2.1544E−03 ...	7438.8	1.9444	0.9020	1.176	0.3035
3.1623E−03 ...	7501.0	2.0506	0.9989	1.179	0.3517
4.6416E−03 ...	7567.3	2.1556	1.0970	1.181	0.4113
6.8129E−03 ...	7637.0	2.2597	1.1960	1.182	0.4845
1.0000E−02 ...	7711.2	2.3601	1.2948	1.182	0.5748
1.4678E−02 ...	7792.8	2.4596	1.3966	1.182	0.6905
2.1544E−02 ...	7885.9	2.5547	1.5014	1.179	0.8440
3.1623E−02 ...	7995.5	2.6461	1.6120	1.174	1.0569
4.6416E−02 ...	8127.0	2.7320	1.7292	1.165	1.3635
6.8129E−02 ...	8287.8	2.8119	1.8550	1.151	1.8268
1.0000E−01 ...	8487.9	2.8831	1.9903	1.128	2.5628
1.4678E−01 ...	8734.7	2.9450	2.1337	1.094	3.7632
2.1544E−01 ...	9035.1	2.9990	2.2825	1.045	5.7382
3.1623E−01 ...	9395.5	3.0435	2.4287	0.980	8.8755
4.6416E−01 ...	9817.3	3.0818	2.5634	0.902	13.343
6.8129E−01 ...	10297.9	3.1178	2.6777	0.824	18.463
1.0000E 00 ...	10838.8	3.1547	2.7688	0.762	22.651
1.4678E 00 ...	11437.3	3.1970	2.8427	0.721	24.747
2.1544E 00 ...	12093.5	3.2507	2.9126	0.700	25.238
3.1623E 00 ...	12804.1	3.3190	2.9888	0.689	25.227
4.6416E 00 ...	13565.4	3.4034	3.0772	0.683	25.521
6.8129E 00 ...	14374.0	3.5016	3.1780	0.680	26.435
1.0000E 01 ...	15233.0	3.6103	3.2894	0.676	28.105
1.4678E 01 ...	16153.1	3.7253	3.4081	0.670	30.498
2.1544E 01 ...	17148.9	3.8432	3.5308	0.664	33.466
3.1623E 01 ...	18245.5	3.9634	3.6555	0.657	36.679

From the two sets of ODFs, we constructed a series of model atmospheres for Vega, using different effective temperatures and gravities. The SSG program currently uses line data for atoms in the first and second stages of ionization. We will discuss in § IV the question of whether lines of doubly ionized species (e.g., Fe III) are important contributors to the line blocking between 2000 and 3000 Å. In Table 2 we give details of the model 9650/3.9/0.0 (the models are identified by $T_{\rm eff}/\log g/[A/{\rm H}]$), which we found gives the best representation of the Vega observational data. Many calculations have been carried out using the model 9650/4.0/0.0, and estimates of the effects of the gravity difference are given when appropriate.

IV. COMPARISON OF MODEL PREDICTIONS WITH OBSERVATIONS

We can compare the predictions of our model atmospheres with the observational data for six separate characteristics: the absolute fluxes at 5556 Å and 10400 Å; the relative absolute fluxes between 3300 and 10800 Å, the region of the ground-based data; the hydrogen line profiles; the curves of growth for various species, such as Fe I, Fe II, and Ti II; the absolute fluxes and line blocking in the ultraviolet; and the infrared fluxes.

The first three comparisons yield information on the temperature of Vega, the fourth establishes the metal abundance, the fifth gives more information on the temperature (this information is less certain than that given by the first three methods because it depends much more on the computed line blocking), and the sixth comparison offers a calibration of the infrared observations, which were taken from aircraft.

Most of the model calculations given in these comparisons have been carried out using local thermodynamic equilibrium (LTE) and the element abundances of Bell and Gustafsson (1978), in particular using 7.4 as the log of the iron abundance. The influence of non-LTE effects on metal lines will be considered later in this section.

Auer and Mihalas (1970) have computed model atmospheres in radiative and statistical equilibrium for various log g and $T_{\rm eff} \geq 12{,}500$ K. Although Frandsen (1974) has made similar calculations for model with log

$g = 4.0$ and $T_{eff} = 10{,}000$ K, Auer and Mihalas presented more detailed results. They found that the continuum features of their $T_{eff} = 12{,}500$ K, $\log g = 4.0$ model in the visible were essentially unaltered by non-LTE effects, and their Table 1 shows no effect for the Balmer jump. The non-LTE Balmer-line calculations have deeper line cores than do the LTE ones, the difference occurring at 0.75 Å from line center for $H\beta$ and $H\gamma$. The departure for Paschen α occurs at 5 Å from line center, the non-LTE line being shallower, and the ratio of equivalent widths is $W(\text{LTE})/W(\text{non-LTE}) = 0.84$ for $P\alpha$ and 0.91 for $P\beta$. The non-LTE calculations for Brackett α show it in emission in the central 3 Å of the profile with an equivalent width of only 4 Å. These calculations will be referred to where appropriate in the following sections but do, of course, refer to a considerably hotter model than is appropriate for Vega.

a) Absolute fluxes at 5556 *Å and* 10400 *Å*

All the calculated fluxes referred to subsequently have been computed using the SSG program. The monochromatic fluxes given by this program typically agree to within 0.2% with the values given by the model atmosphere program MARCS.

The absolute fluxes (F_{5556} and F_{10400}) of the models 9300/4.0/0.0, 9650/3.5/0.0, 9650/4.0/0.0, and 10000/4.0/0.0 are given in Table 3 along with the observed absolute fluxes. The calculated fluxes (in ergs cm^{-2} sec^{-1} Å^{-1}) are averaged over 50 Å band passes and are applicable to both sets of observations since the line blocking is negligible (about 0.1%) in both bandpasses.

TABLE 3

ABSOLUTE FLUXES AT 5556 Å

Model or Observation (Models Denoted by $T_{eff}/\log g/[A/H]$)	Flux (10^7 ergs cm^{-2} s^{-1} Å^{-1})
9300/4.0/0.0	5.13
9650/3.5/0.0	5.59
9650/4.0/0.0	5.61
10000/4.0/0.0	6.06
Tüg, White, and Lockwood (1977)	5.63 ± 0.24
Hayes and Latham (1975)	5.50 ± 0.24
Absolute Fluxes at 10400 Å	
9300/4.0/0.0	0.871
9560/3.5/0.0	0.915
9650/4.0/0.0	0.918
10000/4.0/0.0	0.967
Hayes, Latham, and Hayes (1975)	0.923 ± 0.040
Colors $m(8090) - m(10400)$	
9300/4.0/0.0	−0.689
9650/3.5/0.0	−0.697
9650/4.0/0.0	−0.704
10000/4.0/0.0	−0.716
Hayes, Latham, and Hayes (1975)	−0.703

The F_{5556} values presented in Table 3 suggest the effective temperature is close to 9650 K. The Tüg *et al.* flux gives 9650 K. The Mount Hopkins measurements used by Hayes and Latham give 9650 K and the Mount Palomar meaurements give 9500 K. For the temperature to be as high as 10,000 K, either the angular diameter would have to be too large by 3%, or the flux F_{5556} from Tüg *et al.* too small by 5%, or there would have to be some equivalent combination of these errors. Similarly, the temperature 9300 K is too low, unless corresponding errors occur in the angular diameter and flux. The Hayes, Latham, and Hayes 10,400 Å flux gives $T_{eff} = 9700$ K, but the error bars are such that the observations do not exclude a temperature as low as 9300 K or as high as 10,000 K. The computed flux varies little with changing T_{eff} at the longer wavelength.

b) Relative Absolute Fluxes

The differences between the Hayes and Latham (1975) observed relative absolute fluxes and the theoretical fluxes of the models 9650/4.0/0.0, 9650/3.5/0.0, 10,000/4.0/0.0 are plotted in Figure 3. Both sets of fluxes are normalized to zero at 5556 Å, and the calculated fluxes are integrations over the appropriate band passes. The cooler models give the best overall fit. The differences in the range 3400 to 3636 Å for the hotter model are too large to be acceptable.

The differences between the computed fluxes for the three models and the observed fluxes of Tüg *et al.* also are given in Figure 3. The computed fluxes are integrations over 10 and 20 Å band passes, and the 9650 K models again give the better overall fit. The hotter model is still too bright in the ultraviolet, again by about 0.1 mag. We cannot account for the noticeable dip at 5890 Å; the D lines are not abnormally strong in the calculations. The reason for the discrepancy at 8990 Å is unknown. It is not caused by our omission of the Paschen line P_{10} at 9014 Å. Paschen lines up to P_{18} have been included in the spectrum calculations. These lines must be included to obtain agreement near the Paschen limit. The observed and computed spectra in this region are compared in the next subsection. The computed colors of the models, $m_\lambda(8090) - m_\lambda(10400)$, are given in Table 3, along with the observed color of Hayes, Latham, and Hayes (1975). This observation again indicates $T_{eff} = 9650$ K, but even the very small quoted error of ± 0.01 mag implies an uncertainty of ± 350 K.

The differences in ultraviolet fluxes between the models 9650/3.5/0.0 and 9650/4.0/0.0 are typically 0.03 mag. The comparisons in Figure 3 show that it is not possible to say that one model fits the observations better than the other. In other words, the model results do not yield the log of surface gravity to a precision of better than about ± 0.5 from the relative absolute fluxes, even when the temperature is precisely known. It is,

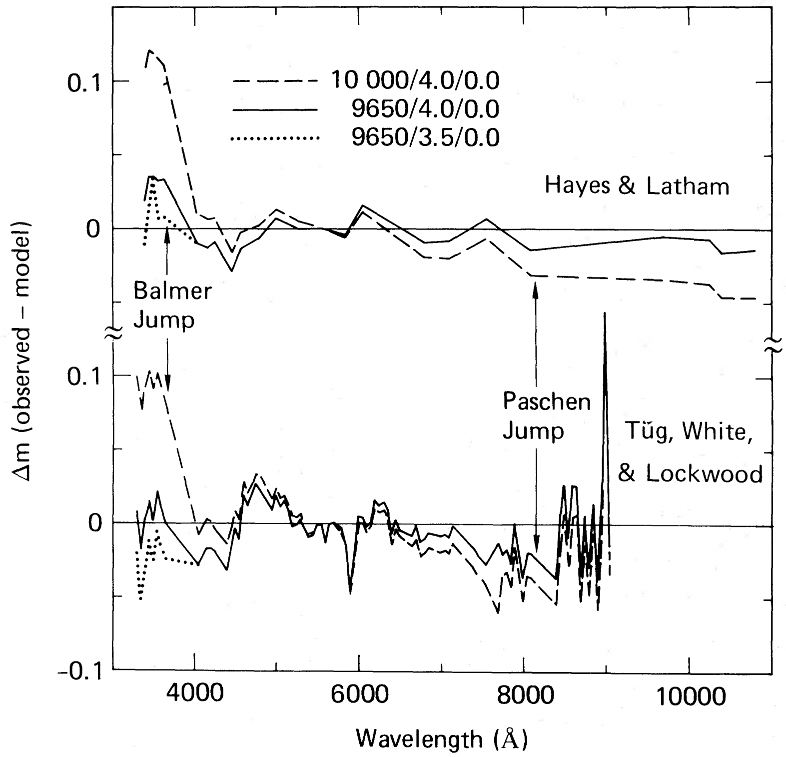

FIG. 3.—The magnitude differences between the Vega models and the observations of Hayes and Latham (1975) and Tüg, White, and Lockwood (1977). The model fluxes have been computed for the same pass bands and at the same wavelengths as were used by the observers, and the individual differences have been joined by smooth lines. Over most of the spectrum, the model 9650/3.5/0.0 corresponds to the model 9650/4.0/0.0.

however, possible to say that no model with $T_{\rm eff} = 10{,}000$ K can fit the observations with any plausible value of log g. Similarly, results we present later suggest that it is not possible to make the model fit the observations by enhancing the metal abundances and consequently increasing the line blocking in the ultraviolet.

The line blocking and emitted fluxes in 50 Å pass bands between 1200 and 12000 Å for the model 9650/4.0/0.0 are given in Table 4. We will use these fluxes in subsequent color calculations. The fluxes in the region of the Balmer limit have been computed by considering only Balmer-line absorption down to $\lambda = 3691.56$ (the central wavelength of H_{16}) and by using this wavelength as the Balmer limit when computing bound-free absorption in atomic hydrogen. Similarly, the Paschen and Brackett limits have been taken as 8430 Å and 15800 Å, respectively.

c) Balmer, Paschen, and Brackett Line Profiles

As stated earlier, the calculations of hydrogen lines for the ODFs have been made using the Edmonds, Schlüter, and Wells (1967, ESW) "modified empirical theory" Stark broadening functions, which have been convolved with Voigt functions that take into account Doppler, natural, and resonance broadening. More recent "unified theory" Stark broadening calculations have been carried out by Vidal, Cooper, and Smith (1973, VCS). Comparison with laboratory experiments indicates that these calculations can be used to give electron densities (N_e) that have an error of at most 5% for $N_e \geq 10^{15}$ cm^{-3}. We define the normal field strength, $F_0 = 1.25 \times 10^{-9} N_e^{2/3}$, and the quantity $\Delta\alpha = \Delta\lambda / F_0$ with $\Delta\lambda$ being the distance from line center. The ratio of the normalized Stark profile $S(\Delta\alpha)$ of the VCS theory to that of the ESW theory for $N_e = 10^{13}$, $T = 10{,}000$ K at $\Delta\alpha = 1.0$, is 0.62, 0.71, and 0.82 for Hα, Hβ, and Hγ, while at $\Delta\alpha = 2.5$ these ratios are 0.67, 0.79, and 0.88. The differences for smaller $\Delta\alpha$ are given by Dreiling (1976). (Note that the ratio of the f value for the Stark components displaced by the electric field to the total f value for the line is included in the VCS $S(\Delta\alpha)$ tables, whereas it is not in the ESW tables.) Since both theories tend to the same Holtsmark wing limit, the ratios become closer and closer to unity as $\Delta\alpha$ increases. In the region of the Vega atmosphere where the hydrogen lines are formed, N_e is such that $\Delta\alpha = 1.0$ corresponds approximately to $\Delta\lambda = 5$ Å. Beyond this distance from

TABLE 4

LINE BLOCKING (η) AND AVERAGE FLUX RADIATED (πF_λ AND πF_ν) (ALLOWING FOR LINE BLOCKING) FOR 50 Å BANDPASSES CENTERED AT THE GIVEN WAVELENGTH

λ	η	πF_ν 10^{-11} W cm-2 Hz^{-1}	πF_λ 10^4 W cm^{-2} μ^{-1}	λ	η	πF_ν 10^{-11} W cm^{-2} Hz^{-1}	πF_λ 10^4 W cm^{-2} μ^{-1}	λ	η	πF_ν 10^{-11} W cm^{-2} Hz^{-1}	πF_λ 10^4 W cm^{-2} μ^{-1}
1225	0.992	0.0155	0.310	4825	0.079	6.12	7.88	8425	0.072	3.61	1.53
1275	0.775	0.132	2.43	4875	0.272	4.79	6.04	8475	0.152	3.77	1.58
1325	0.397	0.357	6.10	4925	0.024	6.35	7.86	8525	0.173	3.65	1.51
1375	0.245	0.450	7.13	4975	0.005	6.41	7.77	8575	0.158	3.68	1.50
1425	0.145	0.527	7.79	5025	0.011	6.32	7.50	8625	0.130	3.78	1.52
1475	0.114	0.644	8.88	5075	0.005	6.29	7.33	8675	0.181	3.53	1.41
1525	0.114	0.846	10.9	5125	0.005	6.23	7.12	8725	0.135	3.69	1.46
1575	0.199	0.848	10.3	5175	0.019	6.08	6.82	8775	0.132	3.68	1.43
1625	0.165	0.897	10.2	5225	0.008	6.10	6.70	8825	0.082	3.86	1.49
1675	0.207	0.898	9.60	5275	0.010	6.02	6.50	8875	0.192	3.37	1.28
1725	0.164	0.996	10.0	5325	0.010	5.97	6.32	8925	0.032	4.00	1.51
1775	0.105	1.08	10.3	5375	0.005	5.95	6.17	8975	0.067	3.83	1.43
1825	0.165	1.03	9.25	5425	0.008	5.87	5.99	9025	0.205	3.24	1.19
1875	0.114	1.11	9.44	5475	0.002	5.86	5.86	9075	0.037	3.89	1.42
1925	0.108	1.13	9.16	5525	0.005	5.78	5.69	9125	0.011	3.96	1.43
1975	0.084	1.18	9.10	5575	0.002	5.75	5.55	9175	0.037	3.83	1.36
2025	0.145	1.12	8.23	5625	0.001	5.70	5.40	9225	0.223	3.07	1.08
2075	0.126	1.17	8.18	5675	0.001	5.65	5.26	9275	0.058	3.69	1.29
2125	0.147	1.17	7.77	5725	0.001	5.60	5.13	9325	0.006	3.86	1.33
2175	0.165	1.17	7.39	5775	0.001	5.55	4.99	9375	0.001	3.85	1.32
2225	0.166	1.19	7.19	5825	0.001	5.50	4.86	9425	0.002	3.82	1.29
2275	0.190	1.17	6.80	5875	0.004	5.43	4.72	9475	0.021	3.72	1.24
2325	0.185	1.20	6.68	5925	0.000	5.41	4.62	9525	0.168	3.13	1.04
2375	0.227	1.16	6.18	5975	0.004	5.34	4.49	9575	0.112	3.32	1.09
2425	0.236	1.17	5.98	6025	0.001	5.31	4.39	9625	0.019	3.64	1.18
2475	0.229	1.20	5.90	6075	0.000	5.27	4.28	9675	0.004	3.67	1.18
2525	0.210	1.26	5.93	6125	0.003	5.21	4.16	9725	0.000	3.66	1.16
2575	0.183	1.33	6.01	6175	0.005	5.15	4.05	9775	0.000	3.63	1.14
2625	0.127	1.45	6.30	6225	0.004	5.11	3.96	9825	0.000	3.60	1.12
2675	0.120	1.49	6.23	6275	0.000	5.09	3.88	9875	0.000	3.57	1.10
2725	0.128	1.50	6.06	6325	0.004	5.03	3.77	9925	0.001	3.54	1.08
2775	0.142	1.50	5.86	6375	0.003	4.99	3.68	9975	0.018	3.46	1.04
2825	0.108	1.59	5.99	6425	0.003	4.95	3.60	10025	0.144	2.99	0.894
2875	0.131	1.58	5.73	6475	0.010	4.87	3.49	10075	0.132	3.01	0.891
2925	0.074	1.71	6.01	6525	0.050	4.64	3.27	10125	0.019	3.38	0.989
2975	0.072	1.75	5.92	6575	0.202	3.86	2.68	10175	0.000	3.42	0.991
3025	0.037	1.84	6.04	6625	0.012	4.74	3.24	10225	0.000	3.40	0.974
3075	0.060	1.83	5.80	6675	0.001	4.75	3.20	10275	0.000	3.37	0.958
3125	0.061	1.86	5.70	6725	0.000	4.72	3.13	10325	0.000	3.35	0.942
3175	0.054	1.90	5.66	6775	0.000	4.68	3.06	10375	0.001	3.32	0.925
3225	0.055	1.93	5.56	6825	0.000	4.64	2.99	10425	0.000	3.30	0.911
3275	0.032	2.00	5.60	6875	0.000	4.61	2.92	10475	0.004	3.26	0.892
3325	0.042	2.01	5.46	6925	0.000	4.57	2.86	10525	0.001	3.25	0.880
3375	0.035	2.06	5.41	6975	0.000	4.53	2.80	10575	0.001	3.23	0.866
3425	0.020	2.12	5.41	7025	0.001	4.49	2.73	10625	0.001	3.20	0.851
3475	0.029	2.12	5.28	7075	0.000	4.46	2.67	10675	0.011	3.15	0.829
3525	0.011	2.19	5.29	7125	0.000	4.43	2.62	10725	0.009	3.14	0.818
3575	0.019	2.20	5.17	7175	0.001	4.39	2.56	10775	0.002	3.13	0.810
3625	0.019	2.23	5.08	7225	0.000	4.36	2.50	10825	0.006	3.10	0.793
3675	0.224	2.25	5.01	7275	0.001	4.32	2.45	10875	0.029	3.01	0.763
3725	0.675	2.71	5.87	7325	0.000	4.29	2.40	10925	0.185	2.51	0.630
3775	0.574	3.52	7.41	7375	0.000	4.26	2.35	10975	0.074	2.83	0.705
3825	0.462	4.40	9.03	7425	0.002	4.22	2.29	11025	0.010	3.00	0.741
3875	0.362	5.16	10.3	7475	0.001	4.19	2.25	11075	0.000	3.01	0.737
3925	0.156	6.75	13.2	7525	0.000	4.16	2.20	11125	0.000	2.99	0.726
3975	0.346	5.18	9.84	7575	0.000	4.13	2.16	11175	0.000	2.97	0.714
4025	0.042	7.50	13.9	7625	0.000	4.10	2.11	11225	0.000	2.95	0.703
4075	0.177	6.37	11.5	7675	0.001	4.06	2.07	11275	0.011	2.90	0.684
4125	0.221	5.97	10.5	7725	0.000	4.03	2.03	11325	0.007	2.89	0.677
4175	0.028	7.37	12.7	7775	0.010	3.97	1.97	11375	0.000	2.89	0.671
4225	0.020	7.35	12.4	7825	0.000	3.97	1.95	11425	0.002	2.87	0.660
4275	0.031	7.20	11.8	7875	0.003	3.93	1.90	11475	0.002	2.85	0.649
4325	0.301	5.13	8.23	7925	0.002	3.91	1.87	11525	0.000	2.84	0.641
4375	0.101	6.53	10.2	7975	0.007	3.86	1.82	11575	0.000	2.82	0.631
4425	0.021	7.05	10.8	8025	0.000	3.86	1.80	11625	0.007	2.78	0.617
4475	0.020	6.98	10.5	8075	0.000	3.83	1.76	11675	0.009	2.76	0.607
4525	0.023	6.89	10.1	8125	0.000	3.80	1.73	11725	0.003	2.75	0.601
4575	0.015	6.87	9.85	8175	0.003	3.76	1.69	11775	0.006	2.73	0.590
4625	0.007	6.86	9.62	8225	0.006	3.72	1.65	11825	0.005	2.71	0.582
4675	0.004	6.81	9.35	8275	0.000	3.72	1.63	11875	0.006	2.69	0.573
4725	0.007	6.73	9.04	8325	0.003	3.68	1.59	11925	0.000	2.69	0.568
4775	0.011	6.63	8.72	8375	0.005	3.65	1.56	11975	0.003	2.67	0.558

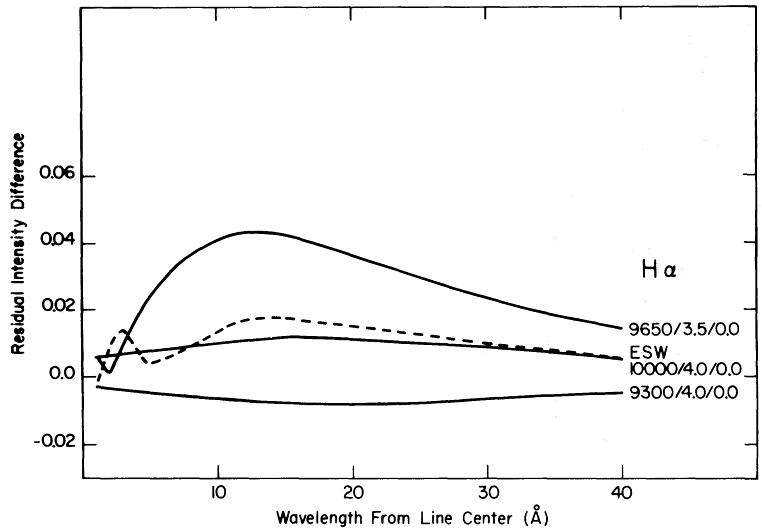

FIG. 4.—The differences in the residual intensity, specified model—9650/4.0/0.0—are plotted versus λ for Hα. The difference between the residual intensities of the VCS and ESW theories are also plotted.

line center, the VCS theory would be expected to give profiles very little different from the ESW theory, at least for Hβ and Hγ, since $S(\Delta\alpha)$ depends approximately on $\Delta\alpha^{-5/2}$.

This prediction is born out by calculations for Hα, Hβ, and Hγ. In Figures 4, 5, and 6 we give the line profiles for the models 10,000/4.0/0.0, 9650/3.5/0.0, and 9300/4.0/0.0 using the VCS theory and for the model 9650/4.0/0.0 using the ESW theory. Resonance and natural broadening have been added to the Stark broadening for Hα. To illustrate the small differences between the profiles, we have plotted the difference between residual intensity and the residual intensity of the 9650/4.0/0.0 model using the VCS theory. The change of the profiles with $T_{\rm eff}$ is seen to be small, as is the difference between the ESW and VCS theories. The change of 0.5 in log g produces an equal or greater change in the profiles than does the change of 700 K in $T_{\rm eff}$.

Peterson (1969) has presented observed profiles of Hα, Hβ, and Hγ for Vega that were corrected for instrumental broadening. Gray and Evans (1973) have observed Hβ and Hγ. References to earlier work are given in both papers. Gray and Evans showed that

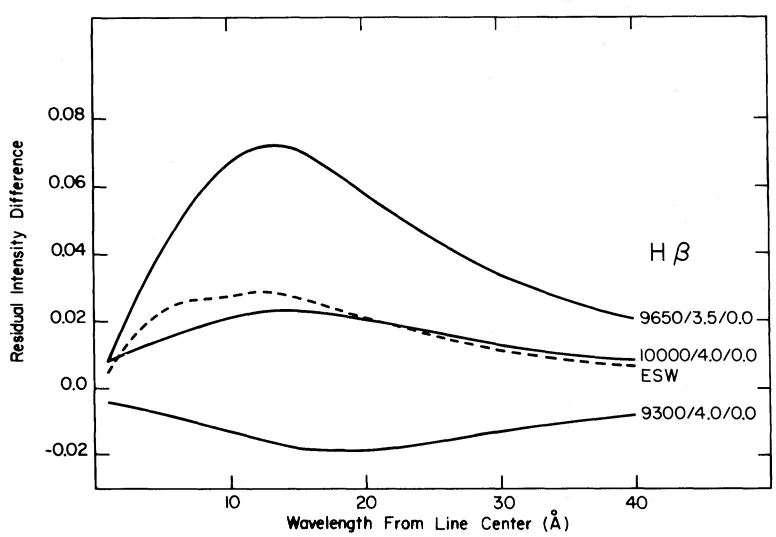

FIG. 5.—As Fig. 4, for Hβ

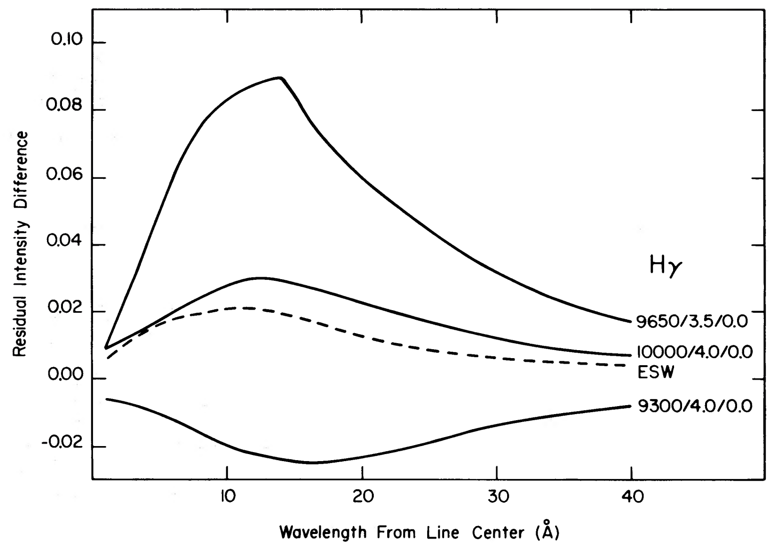

FIG. 6.—As Fig. 4, for Hγ

their results agree very well with those of Peterson. In Figures 7, 8 and 9 we compare our VCS calculated and Peterson's observed profiles. Peterson defined his continuum level as occurring at 70 Å from the line center, and we have normalized our calculations in the same way. The calculated residual intensity at this wavelength is typically 99.5% varying little from line to line or model to model.

Since the change of the profiles with T_{eff} is small, we follow Kurucz (1979) and adopt a value of T_{eff} and use the Balmer lines to find log g. In addition to the profiles themselves, in Figures 7, 8, and 9 we have plotted the difference between residual intensities of the model 9650/3.5/0.0 and 9650/4.0/0.0, as well as the difference observed minus 9650/4.0/0.0. Using the wavelength region 5–20 Å from line center, we find by linear interpolation in log g that Hα gives log $g=3.8$, Hβ gives log $g=4.0$, and Hγ gives log $g=3.9$. Figures 4, 5, and 6 suggest the ESW theory would give log g values about 0.2 greater. It appears that the mean value

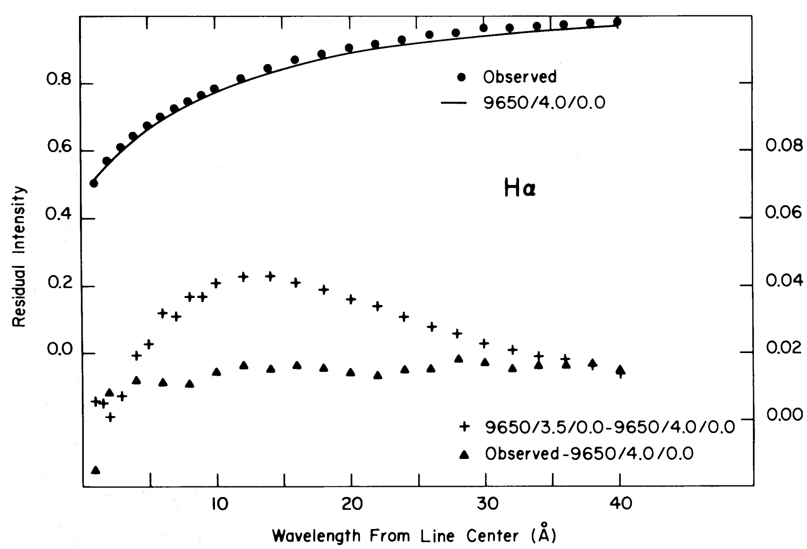

FIG. 7.—Peterson's (1969) observed Hα profile is plotted, as is the profile of the model 9650/4.0/0.0. The difference between these two profiles is also plotted, as is the difference between the models 9650/3.5/0.0 and 9650/4.0/0.0, with the expanded ordinate scale being drawn on the right-hand side of the figure.

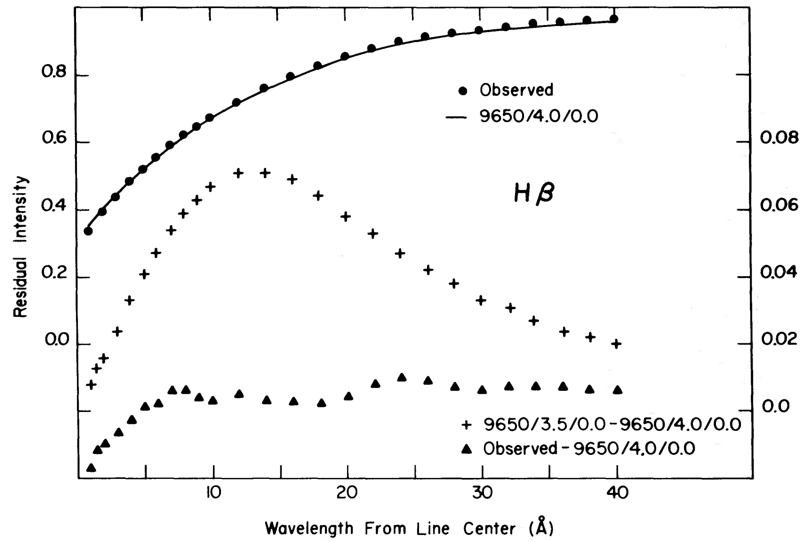

FIG. 8.—As Fig. 7, for Hβ

of log $g = 3.9 \pm 0.2$, in agreement with that deduced earlier from the adopted mass and radius.

The comparison for the wavelength region of the Paschen lines P_{13}, P_{14}, and P_{15} is given in Figure 10. The observations were obtained by J. Tomkin using the McDonald 2.7 m telescope and Tull coudé spectrograph with the 1024 element array. The true continuum is shown for the calculated spectrum, and pseudocontinua are drawn for both calculated and observed spectra. The agreement between calculated and observed values is good.

Using airborne instrumentation, Augason *et al.* (1977) have observed the lines Pα and Pβ. The wavelength resolution ($\lambda/\Delta\lambda$) of these observations is approximately 70. The observed and computed equivalent widths of these lines are given in Table 5. The observed equivalent widths are, in fact, lower limits because they were measured from a Vega-Polaris ratio spectrum. Consequently, the presence of Pα and Pβ in the Polaris spectrum will cause the measured equivalent widths of the Vega lines to be too small.

The Brackett-line profiles of the model 9650/4.0/0.0 are shown in Figure 11, together with the model Pα profile. To facilitate comparison with current infrared data, the calculated spectra have been convolved with a triangular instrumental profile that has a half-width $\Delta\lambda$

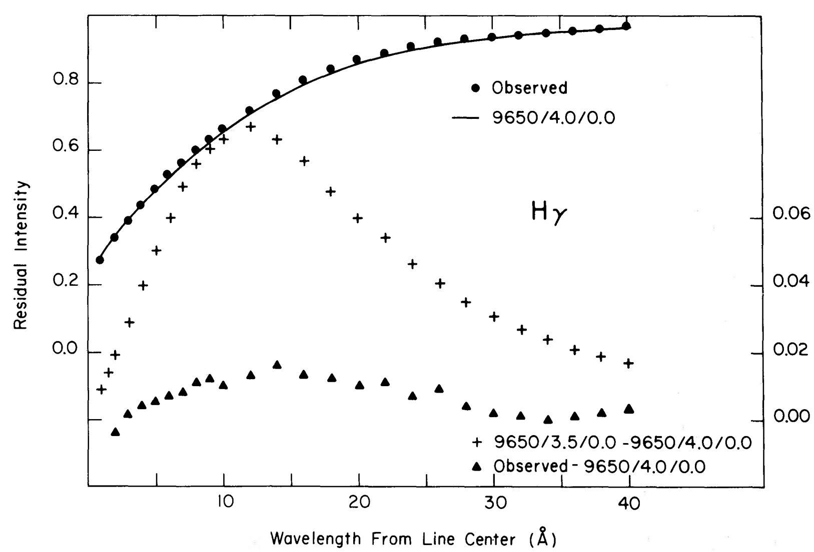

FIG. 9.—As Fig. 7, for Hγ

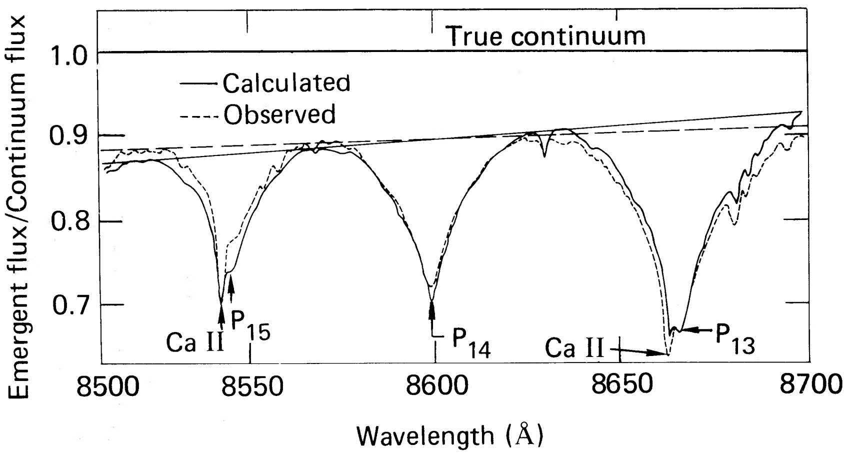

FIG. 10.—The computed Paschen lines and Ca II line profiles compared with observed profiles

given by $\lambda/\Delta\lambda = 70$. The observations of Augason *et al.* (1977) also are plotted in Figure 11, the profiles being obtained by dividing the observed fluxes by the continuum fluxes of the model. Lines up to B_{16} have been included in the calculations. Although the calculated $B\beta$ and $B\delta$ line profiles are in good agreement with the measurements of Augason *et al.* (1977), $B\gamma$ and the higher series lines are about 2% weaker at line center. (This may be due to calibration uncertainties in the observations, since comparison of our calculations and a high dispersion FTS spectrum of Vega obtained at Kitt Peak [Ridgway 1978] gives reasonable agreement for $B\gamma$ and B11.)

Lines of the Pfund series are probably too broad and shallow to be observed. The profile of $L\alpha$ is discussed subsequently (§ IV*e*).

A major reason for our studying the Paschen lines in Vega is that we subsequently compute the colors of our models and we wish to know how reliable these colors are. Obviously the Paschen lines will affect near-infrared colors, such as the Johnson *R* and *I*. Similarly, one reason for studying the Brackett lines was to understand the calibration of the Augason *et al.* data in more detail. In addition, we wished to see if $B\gamma$ was strong enough to affect the narrow band photometry of Cohen, Frogel, and Persson (1978), who use Vega to establish their zero point. The present work suggests $B\gamma$ is not strong enough to affect their measurements.

TABLE 5

PASCHEN LINE EQUIVALENT WIDTHS

$T_{\rm eff}/\log g/[A/H]$	$P\alpha$ (Å)	$P\beta$ (Å)
9650/3.5/0.0.......	11.1	10.6
9650/4.0/0.0.......	13.4	13.2
10,000/4.0/0.0.....	12.7	12.6
Observed	9.0	10.7

d) *Curve-of-Growth Comparison*

We have chosen to analyze the curves of growth from spectra of Fe I, Fe II, and Ti II, restricting ourselves to lines that have equivalent widths greater than $\log W/\lambda = -5.4$ and wavelengths between 4000 and 5000 Å. The scatter in the curves of growth becomes much larger if we include weaker lines. As we have indicated, an effective temperature of 10,000 K seems too hot for Vega, so we chose the model 9650/4.0/0.0 for this analysis. We also compared the results of several models for Fe I.

Very good laboratory oscillator strengths are available for this curve-of-growth analysis from the work of Huber and Parkinson (1972) for Fe I, and Roberts, Anderson, and Sørensen (1973*a*) for Ti II. Huber and Parkinson estimated a maximum error of 25%. The very precise work of Blackwell *et al.* (1979) has confirmed the Huber and Parkinson data. We have used only the Ti II lines for which Roberts, Anderson, and Sørensen quoted an experimental uncertainty of $\leq 25\%$.

The laboratory oscillator strengths for Fe II are less adequate in terms of number of lines, so we used a different method to obtain the curve of growth. First, the Fe II curve of growth was calculated for the HSRA solar model (Gingerich *et al.* 1971), using a logarithmic iron abundance of 7.6 on the usual scale of $\log N(\mathrm{H}) = 12.0$. A Doppler-broadening velocity (DBV), including both thermal and microturbulent terms, of 1.4 km s^{-1} was used, corresponding to the low values of microturbulence found in recent solar-abundance work (Blackwell *et al.* 1976; Biémont, Grevesse, and Huber 1978). This solar Fe II curve of growth was then used to obtain log *gf* values for the Fe II lines used in the Vega analysis, using equivalent widths from Moore, Minnaert, and Houtgast (1966). The log *gf* values found are slightly smaller than the laboratory measurements of Bridges (1973) and of Baschek *et al.* (1970), the

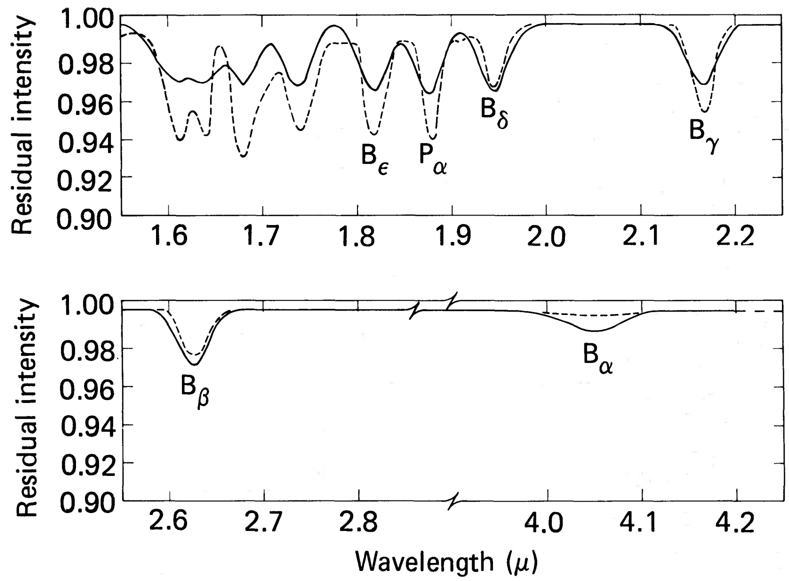

FIG. 11.—The computed profiles of Brackett lines for the model 9650/4.0/0.0 (*solid line*) compared with the observations of Augason *et al.* (1977). Pα is also visible. The calculations have been convolved with an instrumental profile having half-width $\Delta\lambda$ given by $\lambda/\Delta\lambda = 70$.

mean differences being -0.20 (from five lines in common) and -0.05 (from eight lines), respectively. Alternatively, it could be said that the five lines used from the Bridges data give a logarithmic solar iron abundance of 7.4 and the eight Baschek *et al.* lines give 7.55. The values of the oscillator strengths used for the individual lines are given in Table 1.

Hauge and Engvold (1977) recommended values of 4.8 and 7.6 for the solar Ti and Fe abundances, respectively. Their compilation does not include these recent values of Ti: 4.83 (Ellis 1976) and 4.98 ± 0.15 (Whaling, Scalo, and Testerman 1977). Recent calculations for Fe I (Blackwell *et al.* 1979) give values between 7.50 and 7.77, depending on which model atmosphere is used; Biémont and Grevesse (1975) have obtained 7.57 ± 0.11. Baschek *et al.* (1970) found 7.63 ± 0.20 from their own data for 14 Fe II lines. Biémont (1978) found 4.99 ± 0.16 and 7.65 ± 0.15 from Ti II and Fe II lines, respectively.

The observed Ti II curve of growth for Vega is plotted in Figure 12. The excitation temperature was $\theta_{exc} = 0.63$, obtained from the model 9650/4.0/0.0. The LTE theoretical curve of growth from this model also is plotted in Figure 12 and was computed using a titanium abundance of 4.7 and a DBV of 2.5 km s^{-1}. This curve of growth gives a good fit to the observational data, implying that the titanium abundance is close to 4.7.

The observed Fe I and Fe II curves of growth for Vega are plotted in Figures 13 and 14, the excitation temperature again being $\theta_{exc} = 0.63$. The LTE Fe I curves of growth of the models 9650/4.0/0.0, 9650/3.5/0.0, and 10,000/4.0/0.0 are also shown in Figure 13. These curves of growth have been computed using an iron abundance of 7.5 and a DBV of 2.5 km s^{-1}. The computed lines are much stronger than the corresponding observed lines. The Fe I curve of growth of the model 9650/4.0/0.0 implies an iron abundance of 6.9, lower than the solar value. The model 9650/3.5/0.0 gives 7.0. The curve of growth of the hotter model

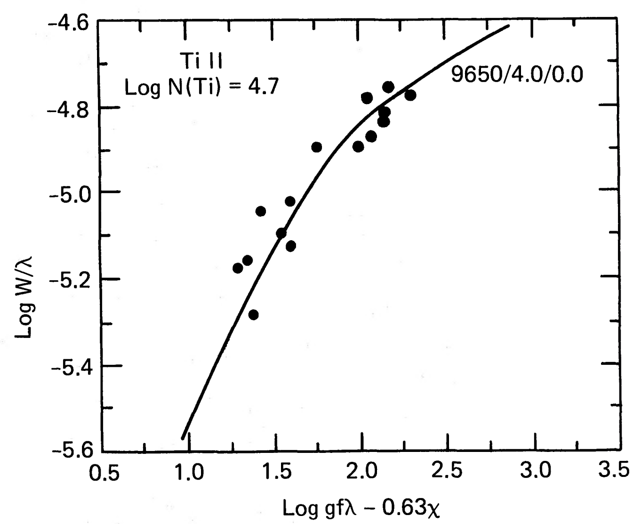

FIG. 12.—The observed Ti II curve of growth compared with that computed from one model using a logarithmic titanium abundance of 4.7.

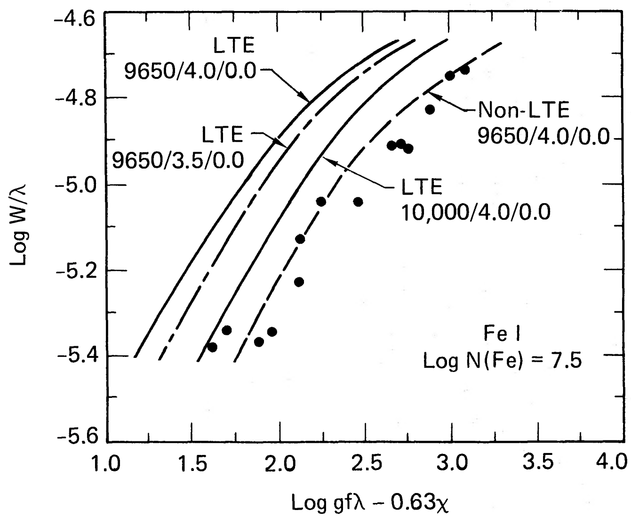

FIG. 13.—The observed Fe I curve of growth together with the LTE curves of growth for three models and the non-LTE curve of growth for model 9650/4.0/0.0. All curves of growth were computed using a logarithmic iron abundance of 7.5.

10,000/4.0/0.0 does give an iron abundance of 7.2, which is closer to the solar value, because of the greater ionization of iron in this model. However, as shown earlier, the fluxes observed just short of the Balmer limit rule out a temperature of 10,000 K for Vega.

The Fe II lines plotted in Figure 14 have $4416<\lambda<4670$ Å, and this relatively narrow interval gives a good sample of lines. The Fe II curve of growth of the model 9650/4.0/0.0 is plotted also for abundances of 7.5 and

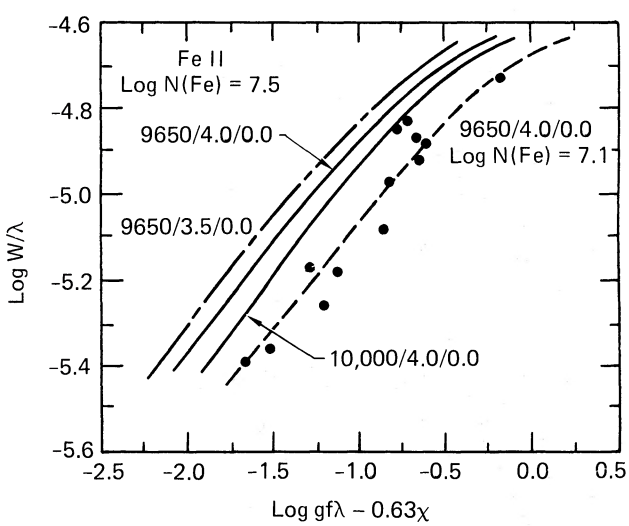

FIG. 14.—The observed Fe II curve of growth together with the LTE curves of growth for three models computed using a logarithmic iron abundance of 7.5. Another LTE curve of growth for 9650/4.0/0.0, this one computed for a logarithmic iron abundance of 7.1, is also shown.

7.1. The computed Fe II lines for an abundance of 7.5 are again stronger than the corresponding observed lines. The non-LTE effects that are expected to be important for the weaker Fe I lines affect primarily the ionization and not the excitation of iron. Because iron is almost completely ionized in Vega, the iron abundance deduced from weak Fe II lines (and the titanium abundance from Ti II lines) should not be affected by departures from LTE, as long as the excitation equilibrium of the ions also follows the Boltzmann distribution. This seems reasonable in view of the Fe I results discussed below. From the Vega Fe II lines in Figure 14, we deduce an iron abundance of 7.1.

Four of the Fe II lines used appear blended to some extent in the solar spectrum. This blending does not appear to make the lines unusable for the purposes of the present paper, since the blended lines were not separated from the unblended ones in a plot of central residual intensity in the solar spectrum versus log $gf\lambda - \chi$ (the residual intensities were measured from the Kitt Peak Solar Atlas [Brault and Testerman 1972] and the excitation temperature of the HSRA is 5040 K). However, we plotted a curve of growth for Fe II lines using log $gf\lambda$ values from Bridges (1973) and from Baschek *et al.* (1970), the latter values being normalized to Bridges' absolute scale by adding 0.15 (Fuhr 1977). This curve of growth yielded an iron abundance of 6.8. It is not surprising that this is a lower value as we noted earlier that the Bridges data were 0.2 greater than the values deduced from the solar spectrum. If we argue that the oscillator strengths used should give 7.6 as the solar iron abundance, then the consequent reduction of the Bridges values gives 7.0 for the Vega abundance.

We also checked whether lines were blended in the spectrum of Vega by studying the line absorption coefficients used in synthetic spectrum calculations. These calculations indicated that two lines in our original list might be blended and we rejected them from the analysis. Further calculations using damping constants multiplied by a factor of 2 showed changes of log W/λ greater than 0.02 occurred only for lines with log $W/\lambda > -4.6$, i.e., only for lines stronger than any which we analyzed.

The DBV value of 2.5 km s^{-1} has been used, as this gives the best fit for all three species. If the DBV value were reduced to 2.0 km s^{-1}, the abundances of Ti and Fe would be increased by approximately 0.05. An increase of DBV to 3.2 km s^{-1} produces a decrease of 0.1 in both the Fe abundance and the Ti abundance.

The errors in abundances of Fe (derived from Fe II lines) and Ti, as evidenced by the scatter in the curves of growth, the quoted errors in laboratory oscillator strengths and gravity, the DBV, and temperature uncertainties, are estimated as being ± 0.3. Allowing for these errors, it appears that Vega has log $N(\mathrm{Fe}) = 7.1 \pm 0.3$ and log $N(\mathrm{Ti}) = 4.7 \pm 0.3$.

Clearly, it is necessary to compare these results with the solar values. As discussed earlier, there is considerable scatter in the latter, even if only recent results are used. If we regard Biémont's (1978) result for titanium as the most obvious basis for comparison, since he uses the Roberts, Anderson, and Sørensen (1973*a*) *gf* values for Ti II, we find [Ti/H] = −0.3 for Vega. Biémont's (1978) solar Fe abundance of 7.65 also is based on ionized lines and gives [Fe/H] = −0.55 for Vega. Alternatively, Cameron's (1973) meteoritic values as normalized by Biémont, if adopted as the solar values, give [Ti/H] = −0.3 and [Fe/H] = −0.35 for Vega.

It is clearly of interest to examine the size of non-LTE effects and see if they could affect the iron abundance deduced from the Fe I lines. In fact, Vega is a very good star for this kind of test of non-LTE line-formation calculations because we feel its temperature is well established. The earlier results of Athay and Lites (1972), Lites (1973), and Lites and Cowley (1974) have demonstrated non-LTE effects in computations for iron in solar-type stars. In particular, the hot ultraviolet radiation from the deeper layers affects the ionization equilibria. These effects are likely to be greater in hotter stars such as Vega and are being studied by Eriksson, Gustaffson, and Saxner (1978), who, at our request, have studied Vega. Their detailed calculations will be reported elsewhere. Their treatment followed the work of Eriksson and Toft (1979) and the model iron atom used was the 12 level, 5 transition model of Lites (1973). The ultraviolet radiation field used was taken from the catalog of Jamar *et al.* (1976). Their calculations showed significant departures from the LTE ionization equilibrium, whereas departures from the Boltzmann distribution occurred only in the outermost layer of the model and affected only the strongest lines.

We used these results for departures from LTE ionization equilibria to compute a new non-LTE curve of growth for Fe I from the 9650/4.0/0.0 model. This curve also is shown in Figure 13. The Fe abundance deduced from this was log N(Fe) = 7.5, in reasonable agreement with the solar value, as was originally expected, and considerably greater than the value given by the LTE Fe I analysis. However, and more significantly, this value is considerably greater than that given by the Fe II lines. Because the Fe II result should be fairly reliable, this suggests that the computed non-LTE ionization corrections are too large. We are left, however, with the puzzle that the apparent iron abundance of Vega is a little lower than that of the Sun, while the titanium abundance is solar. This unexpected result might possibly be caused by errors in the Fe II oscillator strengths or in the stellar equivalent widths or by departures from LTE for Fe II. Also, the Fe I non-LTE calculations, which give the expected iron abundance, may not be correct. The result of Strom, Gingerich, and Strom (1966), that Vega had a solar iron abundance, was obtained using much less reliable oscillator strengths and equivalent widths than those used here. Further measurements of oscillator strengths, particularly of Fe II lines, would be very valuable for further work on this problem.

An analysis using Hunger's equivalent widths gave a higher DBV, of 3 km s^{-1}, and abundances [Fe/H] and [Ti/H] that were 0.1 greater than these found using our own equivalent widths. Since our equivalent widths became available only after much of this paper had been completed, many of the subsequent results are presented for a DBV of 3 km s^{-1} and the differential effects of changing the DBV to 2.5 km s^{-1} are given.

The equivalent widths of lines of doubly ionized metals have been computed using solar values for the relevant metal abundances, and while individual lines may be visible in the spectrum of Vega, their contribution to the overall line blocking in the ultraviolet is unimportant. The strongest such lines were found, using the Kurucz and Peytremann (1975) line data, to be Ti III lines between 1327 and 1504 Å and Fe III lines between 1680 and 2100 Å. The estimated total equivalent width of the Ti III lines is 0.6 Å and that of the Fe III lines is 1.2 Å, which is negligible.

e) Ultraviolet Fluxes and Line Blocking

We converted the absolute fluxes of Code and Meade (1976) to emergent fluxes at the surface of Vega by using the geometrical dilution of 1.62×10^{16}. We then computed the ratios of the emergent fluxes of the model atmospheres in 20 Å bandpasses to these observed fluxes for the wavelength interval 1260 Å $\leq \lambda \leq$ 3200 Å. The results are plotted in Figure 15 for the three models. The line blocking of the model 9650/4.0/0.0 is plotted in Figure 16, along with a schematic representation of some line-blocking measurements (Faraggiana, Hack, and Leckrone 1976). The line blocking of the model 9650/3.5/0.0 is typically 0.015 smaller than that of 9650/4.0/0.0.

Turning to the line-blocking measurements first, we see that in the wavelength interval 1200–1450 Å the agreement between theory and observation is very good. The blocking in this wavelength interval is primarily contributed by Lα. We have included the absorption coefficient of this line in the calculations up to 1416 Å, but it appears to be observable even further from line center than this.

The observed line blocking between 2000 and 3000 Å is typically 10%. The computed line blocking is larger than this, peaking at a value of about 25% around 2450 Å. The line spectrum may well be rich enough to cause measurements of line blocking from *Copernicus* data to be low, owing to uncertainties in continuum location. Detailed comparisons of observed and calculated spectra (discussed subsequently) show good agreement, supporting the calculated line-blocking values.

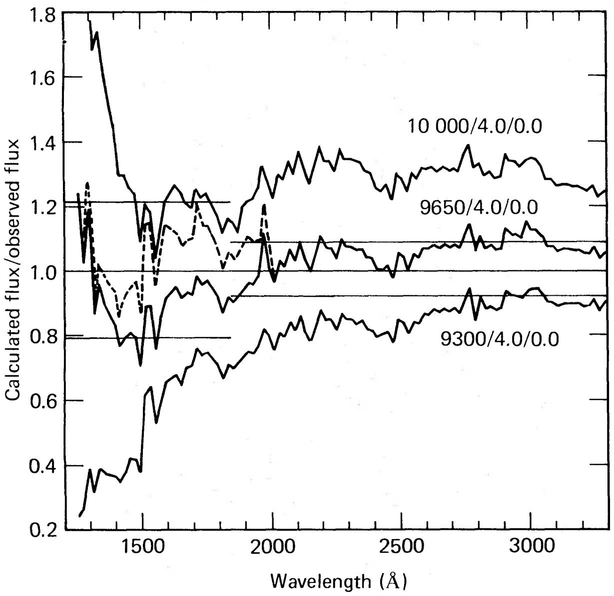

FIG. 15.—The solid lines represent the ratio of calculated-to-observed flux in 20 Å pass bands as a function of wavelength. The dotted line represents the ratio for the 9650/4.0/0.0 model after applying Bohlin's (1978) corrections to the observations. The observed flux was taken from Code and Meade (1976). The distances between the horizontal lines indicate the estimated errors of the observations.

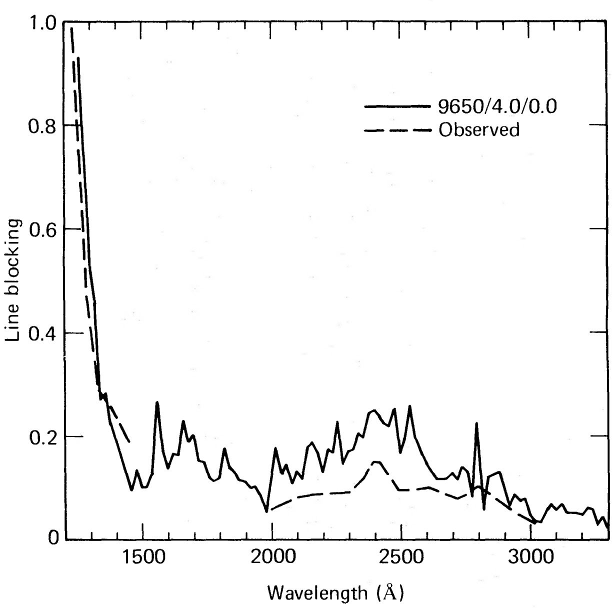

FIG. 16.—Line blocking of the model 9650/4.0/0.0 as a function of wavelength. The pass bands are 20 Å wide. The dashed lines schematically illustrate the line blocking measured by Faraggiana *et al.* (1975).

We calculated the flux ratios shown as solid lines in Figure 15. The Code and Meade error limits of $\pm 8.5\%$ for $1850 < \lambda < 3300$ Å and $\pm 21\%$ for $\lambda < 1850$ Å are also shown. The model 9650/4.0/0.0 gives a respectable fit to the observations. For only four of the twenty-nine 20 Å passbands below 1850 Å does the ratio of calculated to observed flux vary more than 0.21 from 1.00. (The model 9650/3.5/0.0 is about 1% fainter than 9650/4.0/0.0, except in the wing of Lα, where it is perceptibly brighter.) In the wavelength interval 1850–2500 Å, the model 9650/4.0/0.0 is brighter than Vega by more than 8.5% in only one region. The model 9650/3.5/0.0 is typically 4% fainter than 9650/4.0/0.0 and consequently gives a better fit to observations. In the wavelength regions where the computed line blocking is much greater than the observed, the fit of the models to the observations is not significantly different from the fit where the two are in agreement, also suggesting that the observed line blocking may be low in regions of strong line blocking. The fit of the model 9650/4.0/0.0 to the observations between 2500 and 3300 Å is again reasonably good: in only 10 of the 40 wavelength regions did the ratio of calculated to observed flux exceed 1.085. The lower-gravity model 9650/3.5/0.0 gives an even better fit, the flux ratio exceeding 1.085 in only four wavelength regions.

Bohlin *et al.* (1980) have discussed the absolute calibration of the *IUE* satellite, using the absolute calibration of the *OAO 2*, *TD 1/68*, and *ANS* satellites plus rocket and *Apollo 17* data, as well as model atmospheres. They concluded that the Code and Meade fluxes are generally too great in the region 1200–1900 Å, by up to a factor of 1.25. If we apply these correction factors to the Vega data, the observed fluxes and the fluxes of the model 9650/4.0/0.0 are in good agreement between 1200 and 3000 Å. This can be seen in Figure 15, the dotted line representing the ratio of 9650/4.0/0.0 flux to the Code and Meade corrected Vega flux.

The only significant absorption edges due to metals seen in our calculations occur at 1240 Å (C I), at 1445 Å (C I, a jump of 0.27 mag), and 1520 Å (Si I, 0.35 mag). Snijders (1977) has argued that non-LTE effects will weaken Si I and C I bound-free absorption coefficients, but the fit of our model to the observations neither confirms nor contradicts this.

A detailed synthetic ultraviolet line spectrum for Vega, calculated using the model 9650/4.0/0.0, is given in Figure 17 for the wavelength intervals 1205–2105 Å and 2105–3005 Å. The strongest metal lines in this spectrum are marked. The great strength of Lα is clear. The apparent emission peak in Lα is produced by the C I absorption edge at 1240 Å, the change in the continuous absorption coefficient being strong enough to produce this noticeable increase in the line blocking at $\lambda > 1240$ Å. Judging from Figure 17, Lα probably could be traced out 300 Å from line center.

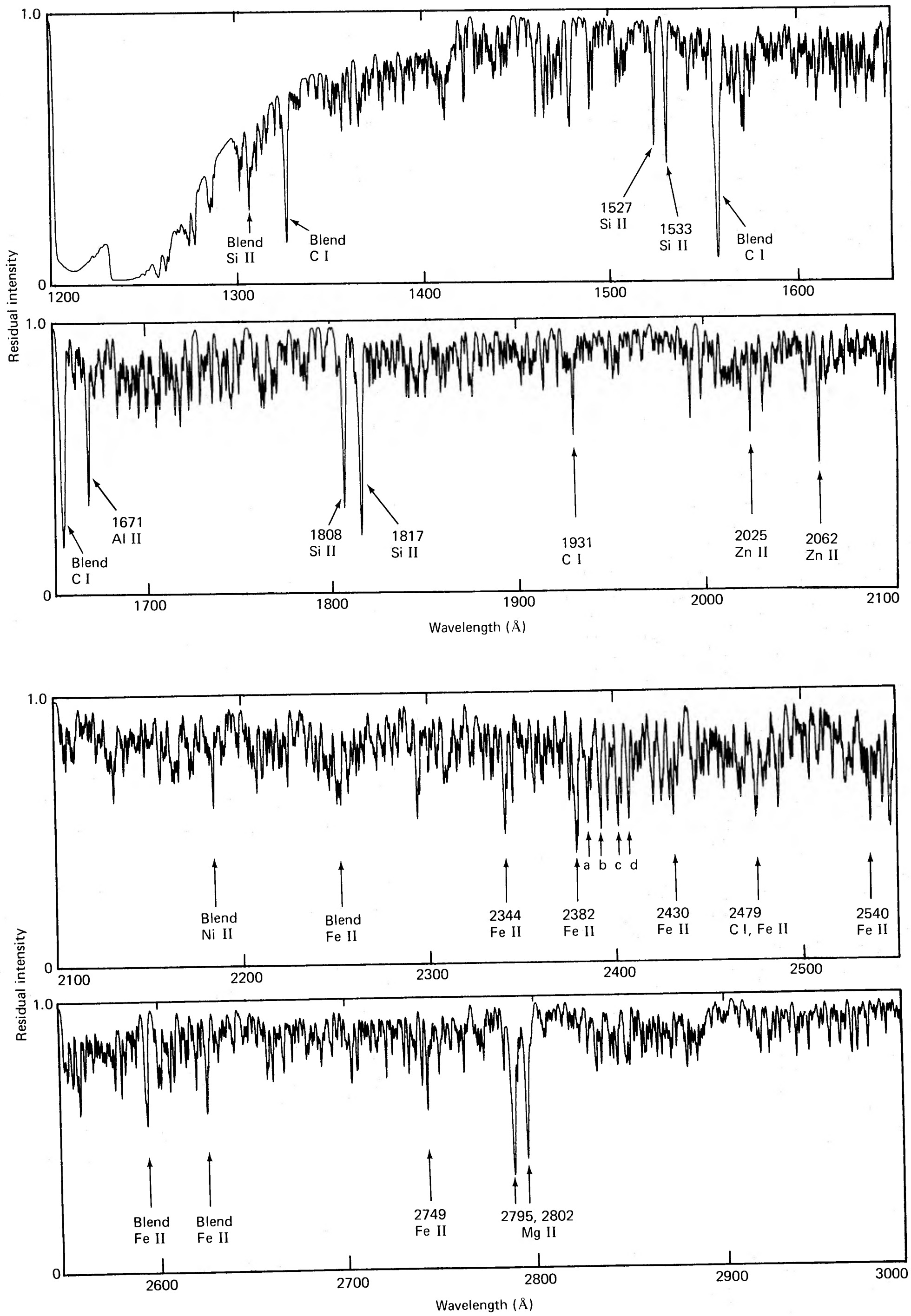

FIG. 17.—The computed ultraviolet synthetic spectrum of the model 9650/4.0/0.0 in the interval 1200–3000 Å. The spectra have been convolved with an instrumental profile of 0.4 Å half-width. The convolution procedure causes the beginning of each spectrum (about the first 3 Å) to be spurious. The apparent emission core in Lyman α is caued by an absorption edge of C I. The lines identified as a, b, c, and d are as follows: a = 2388.6 Å, Fe II; b = 2395.6 Å, Fe II; c = 2404.9 Å, Fe II; d = 2410.5 Å, Fe II.

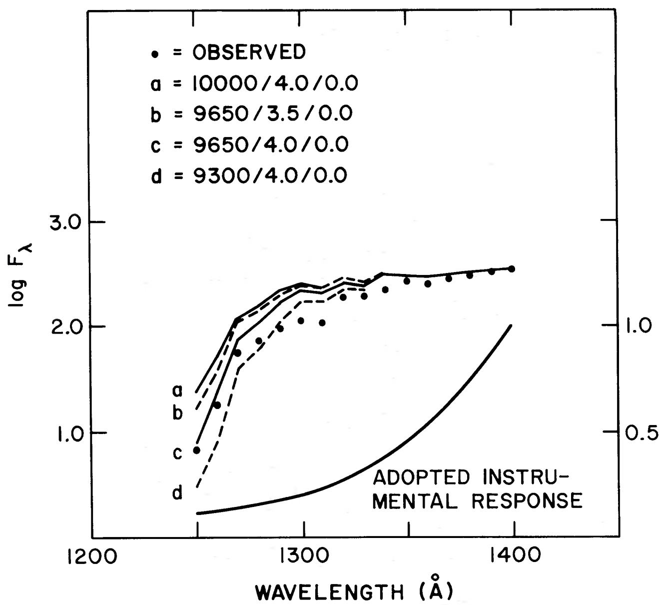

FIG. 18.—The observed and computed fluxes in the region of Lα are shown. The data and adopted instrumental response are from Snow and Jenkins (1977). The calculated profiles are separately normalized to the observations in the interval 1385–1405 Å. The ordinate scale for the instrumental response is on the right hand side of the figure, the units being photons cm^{-2} s^{-1} Å^{-1} per observed counts per 14 seconds.

Copernicus observations can be used as a check on the computed Lα profile although the absolute calibration of the observations is uncertain to about a factor of 2 and the flux from the star is too weak to be observed within ~30 Å of line center. The observed counts of Vega were averaged over 10 Å intervals and converted to fluxes. Both the observational data and the calibration curve were taken from Snow and Jenkins (1977). These fluxes are compared with the calculated fluxes, averaged in the same way, in Figure 18 with the two sets of fluxes being normalized in the interval 1385–1405 Å. The computations were carried out using the ESW theory of Stark broadening plus resonance broadening. (The ESW and VCS Stark broadening theories are equivalent in the line wings, as discussed earlier). The fit between observation and theory for the model 9650/4.0/0.0 seems quite reasonable. Similar work has been carried out by Praderie, Simonneau, and Snow (1975), Aydin and Hack (1978), and Castelli and Faraggiana (1979), who have also discussed the fit of model fluxes to *OAO* and *TD 1* data.

Several extremely strong lines of C I and Si II occur below 2000 Å. A very strong Al II line can also be seen. Above 2100 Å, the strongest lines are mainly Fe II, with some contribution from other singly ionized metals such as Ni II. In Figure 19, we give a detailed comparison of the model spectrum with the *Copernicus* spectrum (taken from Faraggiana, Hack, and Leckrone 1976) for the interval 2595–2635 Å, where a reasonable fit is obtained for the many Fe II lines present. This fit is based on the supposition that the computed and observed continuum levels agree. The fit to Mg II lines is also presented in Figure 19.

In concluding this section, we reiterate that the discussion of the ultraviolet comparison can be reversed. In view of the good fit that the models with $T_{\rm eff}=9650$ K give in the visible and the resonable fit shown in Figure 19, particularly after applying Bohlin's corrections, the model 9650/4.0/0.0 and observations of Vega could be used for calibrating ultraviolet data obtained with the *OAO*, *TD* 1, and *IUE* satellites.

Finally, we have investigated the effects on results of changes in metal abundance and Doppler-broadening velocity. If we reduce the abundance of all metals by a factor of 2 and also reduce the Doppler-broadening velocity from 3 km s^{-1} to 2.5 km s^{-1}, the mean blocking in the intervals 1500–1600 Å and 2200–2300 Å is reduced from 0.162 to 0.132 and from 0.180 to 0.147, respectively. Consequently, the fluxes of the models in the satellite ultraviolet, presented in Figure 15 and Table 4, may well be too faint by about 3%. This factor is small when compared with the flux differences between the models of different temperatures shown in Figure 15 and is comparable to a change in log g of 0.5. The effect on the model fluxes for wavelengths greater than 3000 Å will be considerably less, simply because the blocking by metal lines is much smaller there (the line blocking being 0.036 between 3300 and 3400 Å).

f) *Comparison of Infrared Fluxes*

The continuous fluxes of the model 9650/4.0/0.0 are given in Table 6 in two different units and as a ratio with the flux of a blackbody with $T=10{,}000$ K. These fluxes are given for wavelengths between 1 and 30 μm. The ratio with the blackbody flux is convenient for interpolation. Also, the assumption that Vega radiates as a blackbody has been used by various observers.

The model 10,000/4.0/0.0 is about 5% brighter than 9650/4.0/0.0 at 1 μm, and about 3% brighter at longer wavelengths. The model 9650/3.5/0.0 is about 1% fainter than 9650/4.0/0.0 at these wavelengths. The Schild, Peterson, and Oke (1971) model of Vega, which has $T_{\rm eff}=9650$ K, is very similar to 9650/4.0/0.0 in terms of infrared fluxes, being about 2% fainter for 1 $\mu m \leq \lambda \leq 2$ μm and agreeing within 1% for 2 $\mu m < \lambda <$ 10 μm.

The systematic deviation of the model infrared fluxes from those of a blackbody is not surprising. Continuous absorption is caused predominantly by atomic hydrogen. With increasing wavelength, the continuous-absorption coefficient increases and the emergent radiation consequently is emitted from cooler regions of the model. The ratio of stellar flux to blackbody flux therefore decreases with increasing wavelength.

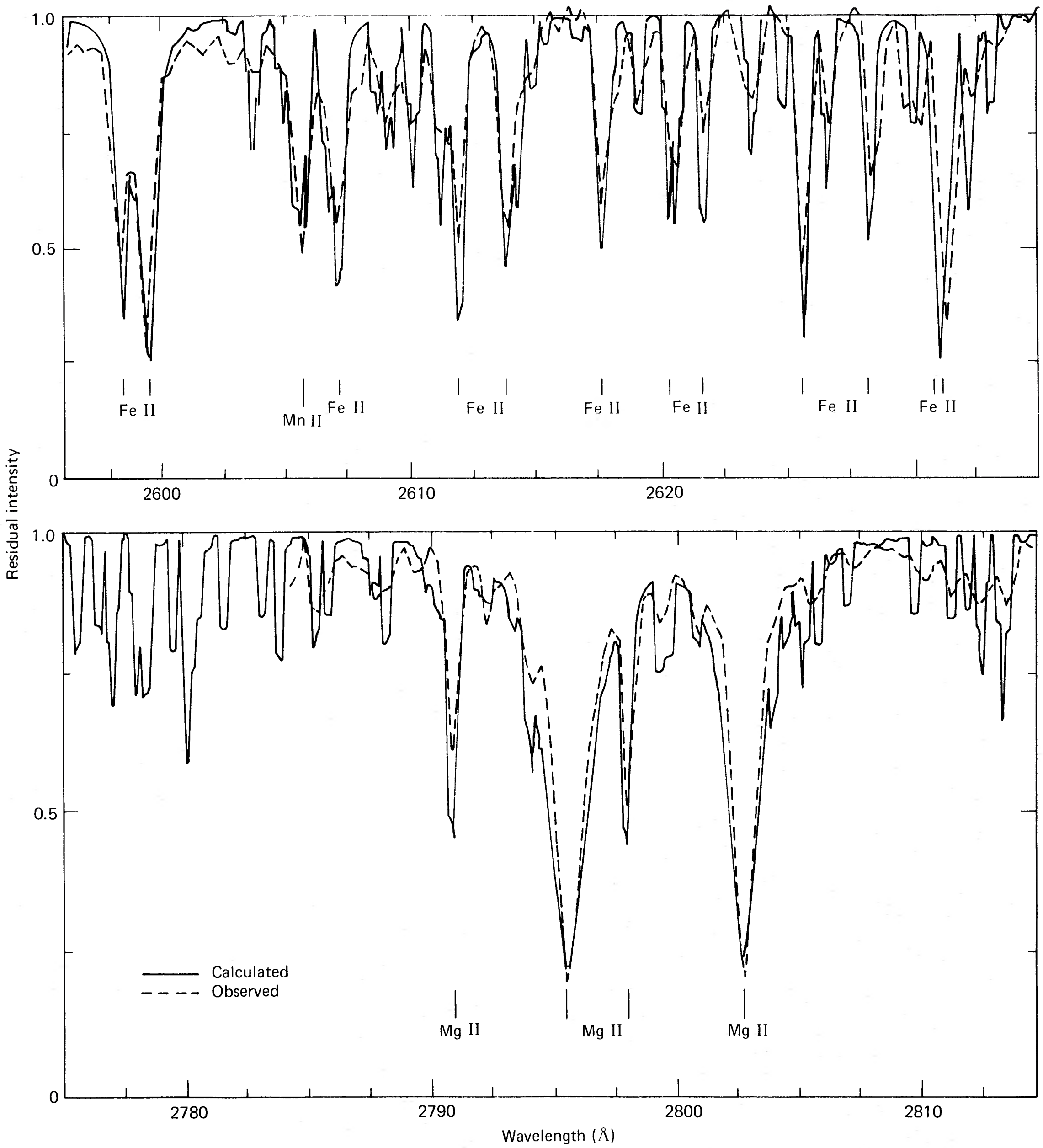

FIG. 19.—*Copernicus* data of Faraggiana *et al.* (1975) compared with the model spectrum for the ranges 2595–2635 Å and 2785–2815 Å. The model used was 9650/4.0/0.0.

Gillett, Merrill, and Stein (1971) gave an absolute calibration of their infrared photometry, wherein Vega is defined to have zero magnitude at all wavelengths. Based on monochromatic flux calculations, rather than integrating over filter passbands, the model 9650/4.0/0.0 gives fluxes of 6.74×10^{-5}, 1.83×10^{-15}, 2.21×10^{-16}, and 7.61×10^{-17} W cm^{-2} μm^{-1} at wavelengths of 3.5, 4.9, 8.4, and 11.0 μm, respectively, for a geometrical dilution of 1.62×10^{16}. These fluxes range from 94% to 88% of the Gillett, Merrill, and Stein (1971) values. The flux at 20 μm is 7.1×10^{-18} W cm^{-2} μm^{-1}, in close accord with the value of 9.7×10^{-18} obtained from the observed 20 μm magnitude for Vega (Morrison and Simon 1973) and the 20 μm magnitude and their adopted absolute flux for Arcturus.

V. MODEL COLORS

Bell and Gustafsson (1978) have computed the colors of the grid of models published by Bell *et al.* (1976). Gustafsson and Bell (1979) have discussed these colors, referring to the colors of an earlier Vega model. The

TABLE 6

CONTINUOUS INFRARED FLUXES OF MODEL 9650/4.0/0.0

μm	πF_λ (W cm^{-2} μm^{-1})	πF_ν (W cm^{-2} Hz^{-1})	$\pi F_\nu/\pi B_\nu$ (for 10,000 K)
1.....	1.048 (+4)	3.510 (−11)	0.9050
1.5 ...	2.499 (+3)	1.874 (−11)	0.8166
2.....	9.118 (+2)	1.216 (−11)	0.8213
2.5 ...	3.964 (+2)	8.259 (−12)	0.8050
3.....	1.974 (+2)	5.923 (−12)	0.7891
3.5 ...	1.091 (+2)	4.456 (−12)	0.7788
4.....	6.513 (+1)	3.474 (−12)	0.7716
4.5 ...	4.125 (+1)	2.784 (−12)	0.7663
5.....	2.737 (+1)	2.281 (−12)	0.7621
5.5 ...	1.887 (+1)	1.903 (−12)	0.7589
6.....	1.343 (+1)	1.611 (−12)	0.7561
7.....	7.335	1.198 (−12)	0.7517
8.....	4.338	9.253 (−13)	0.7483
9.....	2.726	7.359 (−13)	0.7455
10....	1.797	5.991 (−13)	0.7431
15....	3.594 (−1)	2.696 (−13)	0.7342
20....	1.141 (−1)	1.522 (−13)	0.7280
25....	4.678 (−2)	9.747 (−14)	0.7232
30....	2.256 (−2)	6.767 (−14)	0.7195

TABLE 7

COLORS OF VEGA MODELS

		DIFFERENCE[b] BETWEEN OBSERVED AND MODEL ($T_{\rm eff}$/log g/[A/H])		
COLOR	OBSERVED[a] (mag)	9650/3.5/0.0 (mag)	9650/4.0/0.0 (mag)	10000/4.0/0.0 (mag)
UBVRI				
$U-B$ ...	0.00	−0.24	−0.25	−0.19
$B-V$....	0.00	−0.03	0.00	−0.01
$V-R$ ...	−0.04	−0.15	−0.15	−0.14
$R-I$....	+0.03	+0.02	+0.01	+0.03
uvby				
$b-y$	−0.005	−0.016	−0.014	−0.009
m_1......	+0.157	−0.051	−0.017	−0.037
c_1.......	+1.089	−0.142	−0.243	−0.108
JML				
33–52...	−0.022	−0.287	−0.319	−0.201
35–52...	+0.013	−0.187	−0.214	−0.109
37–52...	+0.081	−0.015	+0.073	+0.053
40–52...	+0.015	−0.081	−0.032	−0.049
45–52...	+0.022	−0.006	−0.004	+0.001
52–58...	−0.008	+0.018	+0.021	+0.026
52–63...	−0.023	−0.035	−0.034	−0.025
Geneva				
U.......	+1.505	−0.266	−0.323	−0.207
$B1$......	+0.900	−0.011	+0.012	+0.002
$B2$......	+1.510	+0.014	−0.011	+0.001
$V1$......	+1.662	+0.071	+0.033	+0.044
V.......	+0.959	+0.081	+0.042	+0.053
G.......	+2.168	+0.078	+0.038	+0.047

[a] The observed Vega colors are taken from Johnson *et al.* (1966); Crawford and Barnes (1970); Johnson, Mitchell, and Latham (1967); and Rufener (1974).

[b] Observed minus model.

value of a grid of models is enhanced if reliable theoretical colors are available, because it is then easy to determine which model is appropriate for the analysis of a particular star. For this reason, we have computed the colors of Vega models, basically as a check of the Bell and Gustafsson colors, but also to examine the dependence of color on temperature and gravity for the hotter models. The model calculations are presented in Table 7 in terms of differences (observed minus calculated) between the observed Vega colors and the computed colors for the models 9650/4.0/0.0, 9650/3.5/0.0, and 10 000/4.0/0.0. The color systems considered are *UBVRI*, *uvby*, *Geneva*, and Johnson, Mitchell, and Latham (1967).

Before theoretical colors can be compared with observed colors, the zero points must be established by identifying a particular model with a particular star. We follow Bell and Gustafsson (1978) and use the zero points obtained by identifying the star ϕ^2 Ori with the model 4600/3.0/−0.5. However, the model 9650/4.0/0.0 produces a fit to the observed Vega fluxes that is better than the fit of the cool red-giant models to the fluxes of the corresponding stars, at least in the ultraviolet. Thus, the differences of 0.1 or 0.2 mag in the ultraviolet colors in Table 7 result mainly from error in computed fluxes for ϕ^2 Ori. Possible reasons for this error are discussed by Gustafsson and Bell (1979).

The "thermal" colors ($B-V$, $R-I$, $b-y$, $V1$, V, G, $45-52$, $52-58$, and $52-63$) of Table 7 suggest that the temperature difference between Vega and ϕ^2 Ori is probably greater than 9650–4600 = 5050 K. Increasing this difference makes the computed colors bluer for Vega, if we keep ϕ^2 Ori as the zero-point star. Reducing the gravity of the Vega model improves the agreement of the thermal colors, at the expense of making the differences greater in the ultraviolet. It is tempting to argue, for example, that Vega can be the zero point star and must have $T_{\rm eff}=9650$ K and log $g=4.0$ and that ϕ^2 Ori must consequently be cooler than 4600 K, since this would then improve the agreement of both the thermal and ultraviolet colors for ϕ^2 Ori. However, it would seem more prudent to study ϕ^2 Ori in more detail before doing this.

Despite the improvements that could be made, the differences for the thermal colors are quite small and lend credence to the sensitivity functions used and the neglect of scale factors in the calculations of Bell and Gustafsson. Our detailed treatment of the Vega model in the region of the Paschen limit was carried out, in part, to allow the calculation of accurate $V-R$ and $R-I$ colors. The relatively large observed/calculated difference for $V-R$ may result from an error in the adopted sensitivity function for the Johnson R passband, since calculations for the Cousins $V-R$ system (Bessell 1979) are more satisfactory (see Bell and Gustafsson 1980).

VI. COMPARISON WITH EARLIER RESULTS

Schild, Peterson, and Oke (1971) deduced $T_{\rm eff}=9650$ for Vega on the basis of the relative absolute fluxes of Oke and Schild (1971) and model atmospheres computed allowing for hydrogen line blanketing. In Figure 20 we have plotted the T–τ(5000 Å) relation of their model $T=9650$, log $g=4.05$ and that of our 9650/4.0/0.0 model. It is seen that the inclusion of metal line opacities has introduced the expected surface cooling and that for $0.01 \leq \tau(5000\ \text{Å}) \leq 10.0$ the models are very similar, with our model being backwarmed by at most 100 K at $\tau(5000\ \text{Å})=0.03$. The agreement in the value of $T_{\rm eff}$ deduced is thus not surprising, since the Hayes and Latham (1975) absolute flux calibration is very similar to the Oke and Schild one in the region $4000\ \text{Å} \leq \lambda \leq 9700\ \text{Å}$, the region which has greatest weight in the temperature determination.

We have also compared the T–τ relations of a Kurucz (1979) model $T_{\rm eff}=9500$, log $g=3.9$, solar abundances with our model 9500/3.9/0.0 in Figure 21. The two models are very similar. The *UBV* and *uvby* color tables of Relyea and Kurucz (1978) are based on the temperature and gravity of Vega being defined as 9400 K and log $g=3.95$. Kurucz (1979) shows that his model

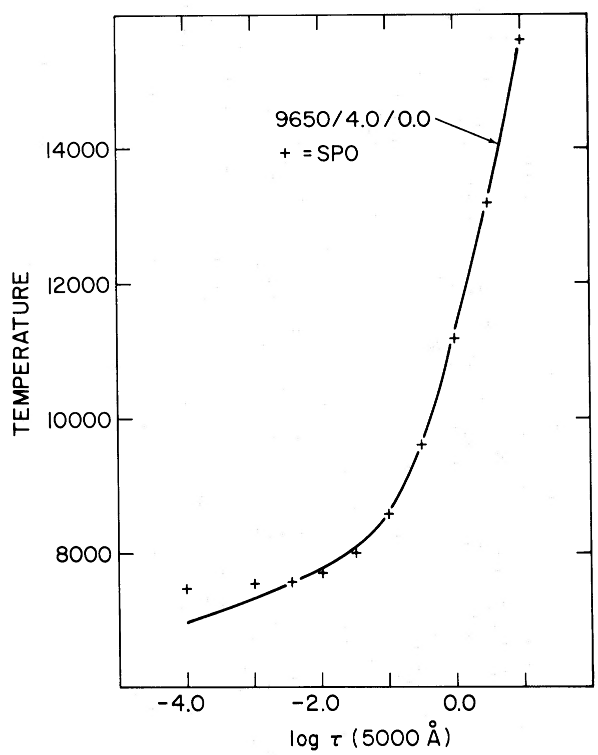

FIG. 20.—The T–τ(5000 Å) relation of our model 9650/4.0/0.0 is compared with the Schild, Peterson, and Oke (1971) 9650/4.0/0.0 model.

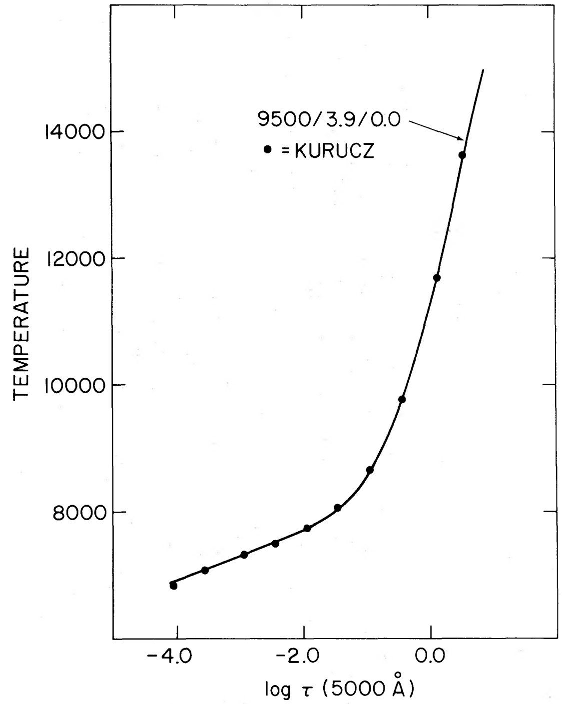

FIG. 21.—The T–τ(5000 Å) relation of our model is compared with the corresponding Kurucz (1979) model.

with these parameters gives a gives a good fit to the relative absolute fluxes of Hayes and Latham and Tüg *et al.* and the hydrogen line profiles of Peterson. A similar comparison with the Hayes and Latham fluxes was given by Kurucz (1975). While the fit of the model to the observations is good, we note that the model is fainter than the star for 4000 Å $\leq \lambda \leq$ 4500 Å where a slightly hotter model would give a better fit.

Code *et al.* (1976) obtained $T_{\text{eff}} = 9660 \pm 140$ K for Vega, based on the angular diameter and *OAO* 2 and ground based observations, which have been integrated to give the absolute flux from the star. The correction to the ultraviolet flux suggested by Bohlin *et al.* (1980) would reduce this temperature by 40 K.

VII. CONCLUSIONS

On the basis of the absolute flux of Vega at 5556 Å and the relative absolute fluxes between 4000 and 9000 Å, we conclude that the effective temperature is 9650 K. The errors in the absolute flux suggest a temperature error of ± 200 K. If the temperature is 9650 K, the relative absolute fluxes between 3295 and 3645 Å suggest log $g = 3.75$, with the uncertainty in absolute flux calibration causing an error of about ± 0.25 in log g. Balmer line profiles suggest the gravity is 3.9 ± 0.2. Both these values agree with the value deduced from the radius and assumed mass, to within the errors.

The Ti II lines in the Vega spectrum yield a logarithmic Ti abundance of 4.7, possibly slightly less than the solar value. The Fe II lines give an abundance of 7.1, somewhat lower than the currently accepted solar value of 7.6. The Fe I lines indicate an iron abundance of 6.9 when LTE calculations are used. Non-LTE effects in the ionization of iron are probably significant enough to give an iron abundance that is 0.6 larger than that given by the LTE work. More accurate measurements of Fe II oscillator strengths would be valuable for further study of this question.

The agreement between observed and computed fluxes between 1260 and 3000 Å is satisfactory. The next problem to be examined here is the detailed comparison of computed line spectra with observed spectra over a wide wavelength interval.

The Vega model 9650/4.0/0.0 gives infrared fluxes that agree with the fluxes of the Schild, Peterson, and Oke (1971) model. Presently, these fluxes should offer a good calibration of flux measurements between 1 and 10 μm.

A further ground-based observation that would be valuable is the measurement of the Vega relative absolute fluxes over a continuous wavelength interval between the ultraviolet and the infrared. There is presently no reason not to measure fluxes in regions of strong lines. It would be interesting to see the accuracy of the model predictions between, say, 3695 and 4045 Å, a region not observed by Tüg, White, and Lockwood (1977). Such measurements would also be valuable in establishing zero points for the calculation of synthetic colors.

It would have been impossible to write this paper without using the MARCS model atmosphere program, and we are grateful to Drs. B. Gustafsson and Å. Nordlund for permission to do so. We are also grateful to Dr. Gustafsson for discussing the problems of Vega and for permission to quote the results of Eriksson, Gustafsson, and Saxner (1978). Drs. R. E. S. Clegg and J. Tomkin kindly supplied observations of Vega and, Dr. D. L. Lambert generously used some of his telescope time to observe Vega with one of us (R. A. B.). Dr. R. L. Kurucz kindly supplied a tape copy of the atomic line calculations of Kurucz and Peytremann. J. Ohlmacher assisted us with the programming work. We acknowledge the support of the National Science Foundation. The calculations were carried out using the facilities of the Computer Science Center, University of Maryland. Some of this research was carried out while R. A. B. held a National Research Council Senior Research Associateship.

REFERENCES

Athay, R. G., and Lites, B. W. 1972, *Ap. J.*, **176**, 809.
Auer, L. H., and Mihalas, D. 1970, *Ap. J.*, **160**, 233.
Augason, G. C., Strecker, D. W., Witteborn, F. C., Erickson, E. F., and Bailey, W. L. 1977, *Bull. AAS*, **9**, 635.
Aydin, C., and Hack, M. 1978, *Astr. Ap. Suppl.*, **33**, 27.
Banfield, F. P., and Huber, M. C. E. 1973, *Ap. J.*, **186**, 335.
Baschek, B., Garz, T., Holweger, H., and Richter, J. 1970, *Astr. Ap.*, **4**, 229.
Bell, R. A., Eriksson, K., Gustafsson, B., and Norlund, Å. 1976, *Astr. Ap. Suppl.*, **23**, 37.
______. 1980, *M.N.R.A.S.*, **191**, 435.
Bell, R. A., and Gustafsson, B. 1978, *Astr. Ap. Suppl.*, **34**, 229.
Bell, R. A., and Upson, W. L. 1971, *Ap. Lett.*, **9**, 109.
Bessell, M. S. 1979, *Pub. A.S.P.*, **91**, 589.
Biémont, E. 1978, *M.N.R.A.S.*, **184**, 683.
Biémont, E., and Grevesse, N. 1975, *Solar Phys.*, **45**, 59.
Biémont, E., Grevesse, N., and Huber, M. C. E. 1978, *Astr. Ap.*, **67**, 87.
Blackwell, D. E., Ibbetson, P. A., Petford, A. D., and Shallis, M. J. 1979, *M.N.R.A.S.*, **186**, 633.
Blackwell, D. E., Ibbetson, P. A., Petford, A. D., and Willis, R. B. 1976, *M.N.R.A.S.*, **177**, 227.
Bohlin, R. C., Holm, A. V., Savage, B. D., Snijders, M. A. J., and Sparks, W. M. 1980, *Astr. Ap.*, submitted.
Brault, J., and Testerman, L. 1972, *A Preliminary Edition of the Kitt Peak Solar Atlas* (unpublished).
Bridges, J. M. 1973, in *Phenomena in Ionized Gases*, Proc. 11th Conf. Prague, ed. I. Stoll (Prague: Czechoslovak Acad. Sciences), p. 418.
Cameron, A. G. W. 1973, *Space Sci. Rev.*, **15**, 121.
Castelli, F., and Faraggiana, R. 1979, *Astr. Ap.*, **79**, 174.
Code, A. D., David, J., Bless, R. C., and Hanbury Brown, R. 1976, *Ap. J.*, **203**, 417.
Code, A. D., and Meade, M. 1976, *Wisconsin Ap.*, No. 30.
Cohen, J. G., Frogel, J. A., and Persson, S. E. 1978, *Ap. J.*, **222**, 165.
Corliss, C. H., and Bozman, W. R. 1962, US National Bureau of Standards, Monograph No. 53.
Corliss, C. H., and Tech, J. L. 1968, US National Bureau of Standards, Monograph No. 108.
Crawford, D. L., and Barnes, J. V. 1970, *A. J.*, **75**, 978.
Dreiling, L. A. 1976, Ph.D. thesis, University of Maryland.
Edmonds, F. N., Schlüter, H., and Wells, D. C. 1967, *Mem. R.A.S.*, **71**, 271.
Ellis, R. S. 1976, *Solar Phys.*, **50**, 261.
Eriksson, K., Gustafsson, B., and Saxner, M. 1978, private communication.
Eriksson, K., and Toft, S. 1979, *Astr. Ap.*, **71**, 178.
Faraggiana, R., Hack, M., and Leckrone, D. S. 1976, *Ap. J. Suppl.*, **32**, 501.
Frandsen, S. 1974, *Astr. Ap.*, **37**, 139.
Fuhr, G. 1977, private communications.
Garz, T. 1973, *Astr. Ap.*, **26**, 471.
Gehlich, U. K. 1969, *Astr. Ap.*, **3**, 169.
Gillett, F. C., Merrill, K. M., and Stein, W. A. 1971, *Ap. J.*, **164**, 83.
Gingerich, O., Noyes, R. W., Kalkofen, W., and Cuny, Y. 1971, *Solar Phys.*, **18**, 347.
Goly, A., Moity, J., and Weniger, S. 1975, *Astr. Ap.*, **38**, 259.
Gray, D. F., and Evans, J. C. 1973, *Ap. J.*, **182**, 147.
Gustafsson, B., and Bell, R. A. 1979, *Astr. Ap.*, **74**, 313.
Gustafsson, B., Bell, R. A., Eriksson, K., and Nordlund, Å. 1975, *Astr. Ap.*, **42**, 407.
Hanbury Brown, R., Davis, J., and Allen, L. R. 1974, *M.N.R.A.S.*, **167**, 121.
Hauge, O., and Engvold, O. 1977, Institute of Theoretical Astrophysics, Blindern-Oslo, Report No. 49.
Hayes, D. S. 1970, *Ap. J.*, **159**, 165.
Hayes, D. S., and Latham, D. W. 1975, *Ap. J.*, **197**, 593.
Hayes, D. S., Latham, D. W., and Hayes, S. H. 1975, *Ap. J.*, **197**, 587.
Huber, M. C. E. 1974, *Ap. J.*, **190**, 237.
Huber, M. C. E., and Parkinson, W. H. 1972, *Ap. J.*, **172**, 229.
Hunger, K. 1955, *Zs. f. Ap.*, **36**, 42.
Jamar, C., Macua-Hercot, D., Monfils, A., Thompson, G. I., Houziaux, L., and Wilson, R. 1976, *Ultraviolet Bright Star Spectrophotometric Catalogue* (Paris: European Space Agency), p. 17.
Jenkins, L. F. 1963, *General Catalogue of Trigonometric Stellar Parallaxes* (New Haven: Yale University Observatory).
Johnson, H. L., and Méndez, M. E. 1970, *A.J.*, **75**, 785.
Johnson, H. L., Mitchell, R. I., Iriarte, B., and Wisniewski, W. Z. 1966, *Comm. Lunar Planet. Lab.*, **4**, 99.
Johnson, H. L., Mitchell, R. I., and Latham, A. S. 1967, *Comm. Lunar Planet. Lab.*, **6**, 85.
Kurucz, R. L. 1975, *Dudley Obs. Rept.*, No. 9, 271.
______. 1979, *Ap. J. Suppl.*, **40**, 1.
Kurucz, R. L., Peytremann, E. 1975, *Smithsonian Ap. Obs. Spec. Rept.*, No. 362.
Lites, B. W. 1973, *Solar Phys.*, **32**, 283.
Lites, B. W., and Cowley, C. R. 1974, *Astr. Ap.*, **31**, 361.
Malaise, D., Gros, M., and Macau, D. 1974, *Astr. Ap.*, **33**, 79.
McCammon, D., Münch, G., and Neugebauer, G. 1966, *Ap. J.*, **147**, 575.
Moore, C. E., Minnaert, M. G. H., and Houtgast, J. 1966, US National Bureau of Standards, Monograph No. 61.
Morrison, D., and Simon, T. 1973, *Ap. J.*, **186**, 193.
Nordh, L. H., Olofsson, S. G., and Augason, G. C. 1978, *A.J.*, **83**, 188.
Oke, J. B., and Schild, R. E. 1970, *Ap. J.*, **161**, 1015.
Panek, R. J. 1977, *Ap. J.*, **216**, 747.
Peach, G. 1970, *Mem. R.A.S.*, **73**, 1.
Peterson, D. A. 1969, *Smithsonian Ap. Obs. Spec. Rept.*, No. 293.
Praderie, F., Simonneau, E., and Snow, T. P. 1975, *Ap. Space Sci.*, **38**, 337.
Relyea, L. J., and Kurucz, R. L. 1978, *Ap. J. Suppl.*, **37**, 45.
Ridgway, S. T. 1978, private communication.
Roberts, J. R., Anderson, T., and Sørensen, G. 1973*a*, *Ap. J.*, **181**, 567.
______. 1973*b*, *Ap. J.*, **181**, 587.
Roberts, J. R., Voigt, P. A., and Czernichowski, A. 1975, *Ap. J.*, **197**, 791.
Rufener, F. 1974, private communication.
Schild, R. E., Peterson, D. M., and Oke, J. B. 1971, *Ap. J.*, **166**, 95.
Snijders, M. A. J. 1977, *Ap. J.*, **214**, L35.
Snow, T. P., and Jenkins, E. B. 1977, *Ap. J. Suppl*, **33**, 269.
Strecker, D. W., Erikson, E. F., and Witteborn, F. C. 1979, *Ap. J. Suppl.*, **41**, 501.
Strom, S. E., Gingerich, O., and Strom, K. M. 1966, *Ap. J.*, **146**, 880.
Travis, L. D., and Matsushima, S. 1968, *Ap. J.*, **154**, 689.
Tüg, H., White, N. M., and Lockwood, G. W. 1977, *Astr. Ap.*, **61**, 679.
Vidal, C. R., Cooper, J., and Smith, E. W. 1973, *Ap. J. Suppl.*, **25**, 37.
Vogt, S. S., Tull, R. G., and Kelton, P. 1978, *Appl. Optics*, **17**, 574.
Warner, B. 1967, *Mem. R.A.S.*, 70, 165.
Whaling, W., Scalo, J. M., and Testerman, L. 1977, *Ap. J.*, **212**, 581.
Wiese, W. L., Smith, M. W., and Glennon, B. M. 1966, *National Standard Reference Data Series*, **4** (Washington: US National Bureau of Standards), p. 6.
Wiese, W. L., Smith, M. W., and Miles, B. M. 1969, *National Standard Reference Data Series*, **22** (Washington: US National Bureau of Standards), p. 6.

R. A. Bell: Code 681, Laboratory for Astronomy and Solar Physics, NASA/Goddard Space Flight Center, Greenbelt, MD 20771

L. A. Dreiling: Lawrence Livermore Laboratory, University of California, Livermore, Ca 94550